

Direct Laser Writing of Fluorescent Silver Nanoclusters: A Review of Methods and Applications

Puskal Kunwar and Pranav Soman*

Cite This: *ACS Appl. Nano Mater.* 2020, 3, 7325–7342

Read Online

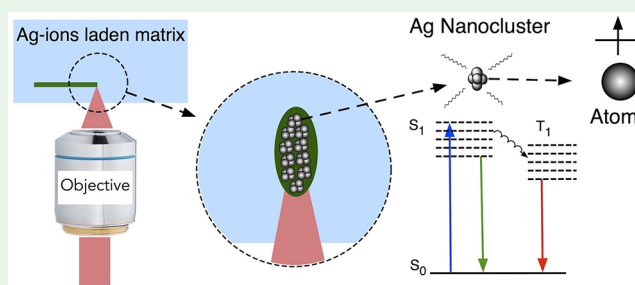
ACCESS |

Metrics & More

Article Recommendations

ABSTRACT: Metal nanoclusters (NCs) are nanomaterials of size of less than 2 nm that exhibit a set of unique physical, chemical, optical, and electronic properties. Because of recent interest in NCs, a great deal of effort is being made to develop synthetic routes that allow control over the NC size, shape, geometry, and properties. Direct laser writing is one of the few synthesis methods that allow the generation of photostable NCs with high quantum yield in a highly controlled fashion. A key advantage of laser-written NCs is the ability to create easy-to-use solid-state devices for a range of applications. This review will present necessary background and recent advances in laser writing of silver NCs and their applications in different solid-state matrixes such as glass, zeolites, and polymer substrate. This topic will be of interest to researchers in the fields of materials science, optics and photonics, chemistry, and biomedical sciences.

KEYWORDS: nanoclusters, silver, direct laser writing, 3D fabrication, fluorescence, photostability



1. INTRODUCTION

Nanotechnology plays an important role in modern society in enabling technologies for applications in information and communication, imaging, sensing, healthcare and energy, among others.¹ In recent years, “metallic nanoclusters (NCs)” and their applications have emerged as an active area in nanotechnology research.² Metallic NCs represent a new class of luminescent nanomaterials with metal cores that consist of a few to tens of atoms. They are ultrasmall materials with size of less than 2 nm, and they exhibit a quantized energy level that gives rise to significantly different optical, electrical, and chemical properties compared to their larger nanoparticle (NP) counterparts. They seem to act as a missing link between individual metal atoms and larger NPs.^{3–8}

NC history dates back to prehistoric times. For instance, the C₆₀ carbon NCs are suggested to have formed during the creation of the universe.^{7,9} Scientific studies on the NCs can be traced back to the 1950s and 1960s, where they were formed from intense molecular beams at low temperature by supersonic expansion.⁷ Later, laser-assisted techniques made it possible to create NCs of a vast majority of elements in the periodic table.¹⁰ Ever since, there have been significant amounts of work done on NCs of noble metals, semiconductor elements, and compound NCs.^{5,7}

In recent years, NCs are most commonly synthesized and studied in solvated form.^{2,8} Effort has been made to develop easy synthetic strategies to precisely control the number of atoms and size of the NCs. Already, several methods have been

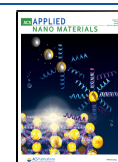
developed to synthesize stable NCs in a scalable manner.^{3,10–24} Furthermore, researchers have used surface chemistry to generate NCs with tunable properties such as photoluminescence, surface-enhanced Raman scattering (SERS), and electrochemiluminescence.^{3,14,17,26,27} They have been functionalized with organic, inorganic, biological, and polymeric molecules such as thiols, amino acids, dendrimers, DNA, and zeolites, which serve as scaffolds to stabilize NCs and prevent them from forming larger NPs.^{3,11,17–19,24,25,28–31} Among the properties of NCs, photoluminescence has gained utmost attention because the fluorescence obtained from NCs, in most cases, is photostable and bright with a large Stokes shift and exhibits tunable emission.^{4,8,32–34} The nontoxic properties and ultrasmall size of NCs have made them better candidates for biological imaging applications compared to organic dyes and quantum dots.^{3,8}

Because there are many reviews on the theoretical and experimental aspects of NCs, we will focus on the synthesis and fabrication of user-defined NC structures using direct laser writing (DLW) in this review article.^{2,4–6,8,35,36} DLW has been used as a promising method to synthesize NCs in solid

Received: May 15, 2020

Accepted: July 13, 2020

Published: July 13, 2020



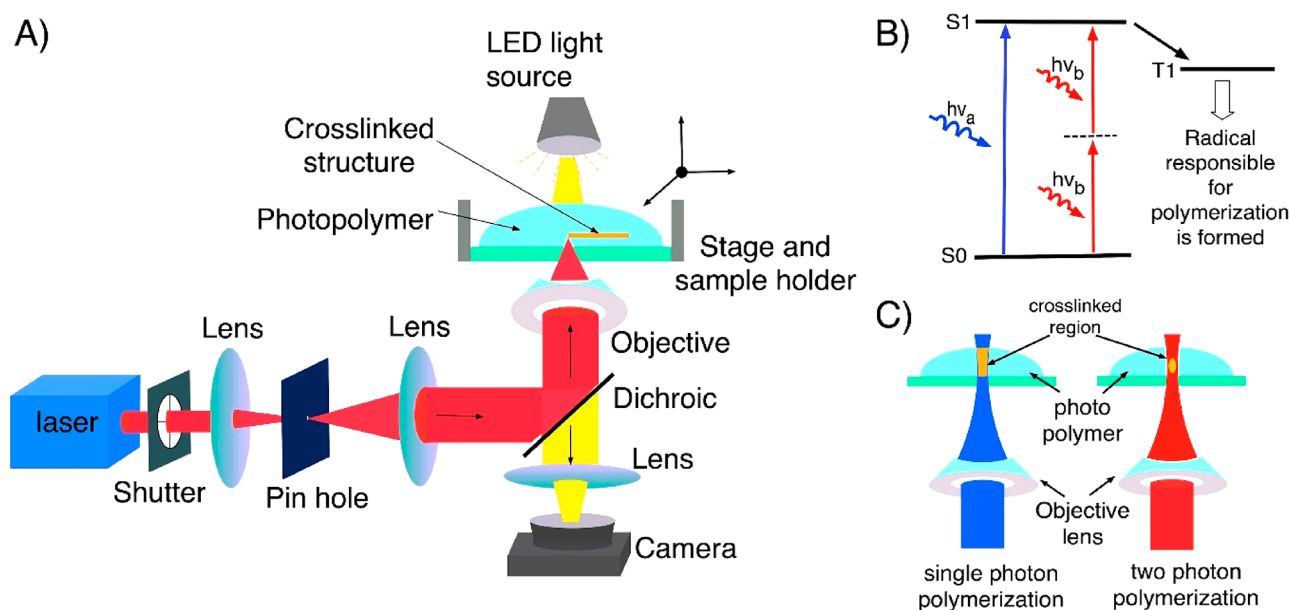


Figure 1. (A) Optical setup of DLW consisting of a laser source, beam guiding and focusing optics, sample holder and scanning stage, and a microscopy arm for observing the writing process. (B) Diagram depicting the energy transitions in single-photon absorption and TPA. (C) Schematic showing the single-photon-absorption- and TPA-induced DLW of a photopolymer. Single-photon polymerization (left) occurs in the entire area of the photopolymer exposed to UV/visible light, and two-photon polymerization (right) results only in the focal point of the laser beam because of the simultaneous absorption of two photons of near-IR light.

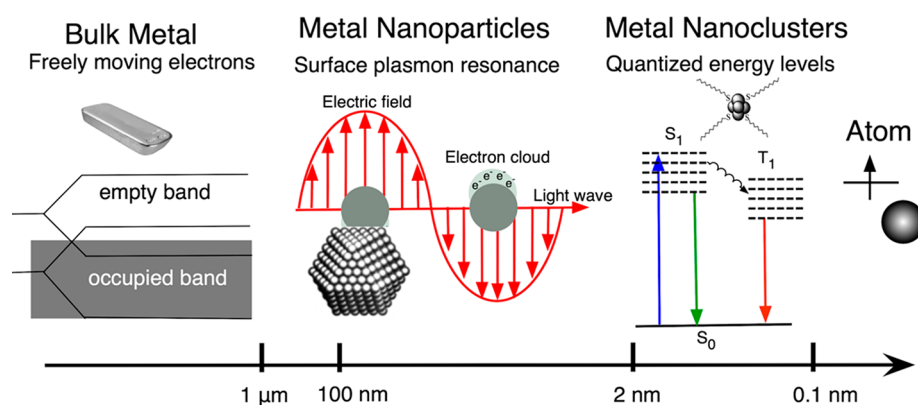


Figure 2. Schematic showing the formation of quantized electronic energy levels on the way from bulk metal to an atom.

substrates that has led to a variety of NC-based functional devices for data storage, labeling, and light-emitting-diode (LED) applications.^{32,33,37–43} Using the case study of silver nanoclusters (AgNCs), this review will first introduce the DLW method, followed by recent advances in methods and applications of laser-written NC structures in different solid-state matrixes.

2. DLW

Advances in manufacturing techniques have enabled the fabrication of simple to complex structures using different materials at different size scales.^{44–47} DLW has emerged as a new manufacturing technology over the past 2 decades that has generated interest in both academic research and industrial applications.^{48–50} DLW has been widely used to fabricate user-defined multiscale structures at a resolution of a few hundred nanometers in the fields of optics and photonics, microfluidics, biomedical engineering, microrobotics, and electronics using a broad range of materials.^{44–46,48–54} In this technique, a laser beam is used to print two-dimensional (2D)/three-dimensional (3D) structures by using different mechanisms such as photopolymerization, photoablation, and laser-induced forward transfer. However, to achieve the submicrometer resolution, a laser beam is focused with an objective lens. The focused laser beam combined with the scanning system can print a microstructure using single-photon- or multiphoton-absorption-induced DLW as explained below (Figure 1A–C).^{55–57}

Single-photon-absorption-induced DLW is a simple way to fabricate one-dimensional (1D)/2D structures that utilize a low-cost continuous-wave (CW) laser operating at a wavelength located within the absorption band of the photosensitive material. In this process, single-photon polymerization occurs within the entire area of the photopolymer that is exposed to light, and therefore this method is limited to planar fabrication (Figure 1B,C).^{55,58} Multiphoton-absorption-induced DLW is a 3D fabrication technique based on nonlinear absorption of light, predominantly reported for two-photon absorption (TPA). The probability of TPA is several orders of magnitude weaker than linear absorption,

which demands a very high light intensity and is delivered by an ultrafast, typically femtosecond, laser. In TPA, the laser-matter interactions occur only at the laser focal spot (Figure 1B,C)^{59,60} which allows the use of longer-wavelength laser beams that can penetrate deep inside the photopolymer, making this method uniquely suited to fabricate 3D structures.⁶¹ DLW has been utilized to print structures using a variety of photosensitive materials such as polymers,⁵¹ biodegradable polymers,^{62–64} hybrid ceramic materials,^{65,66} hydrogel,^{47,53,67–71} proteins,^{67,68} and graphene.^{72–74} Apart from these materials, DLW can also print 2D and 3D metallic microstructures using a polymeric solution containing metal ions.^{72,75} In this process, light is used to photoreduce metal ions to metal NPs, which polymerize to form 3D metallic structures.^{76–78} On this note, Kawata et al. demonstrated femtosecond laser metal printing in an aqueous solution.⁷⁹ Using the technique, Zhao and co-workers performed DLW of a silver aqueous solution to print transparent and highly conductive silver grid electrodes.^{80,81} In another study, Wegener et al. reported conducting gold microstructures by simultaneously polymerizing the polymer and also reducing gold ions from the gold salt.⁸² Further, Stellacci et al. and others have used DLW to fabricate silver metal micro/nanostructures.^{83,84} Recently, DLW-mediated metal NC structures have also been fabricated in substrates made out of specialized glass, zeolites, and polymers.^{32–34,37–39,42,43,85–94}

3. NCs

On the basis of the size and corresponding properties, metal can be divided into bulk metal, metal NPs, and metal NCs (Figure 2).^{7,8,95,96} Bulk metals consist of a sea of free delocalized electrons, which give them metal-like properties such as high electrical and thermal conductivity, mechanical ductility, and surface luster, whereas NPs are characterized by the collective oscillation of electrons, i.e., surface plasmons.^{8,97} Further, a decrease in the size of the metal particles to the Fermi wavelength of the electron gives rise to metal NCs; a multiatom particle with significantly different optical, electrical, and chemical properties compared to their larger counterparts. These entities are molecule-like species with discrete energy levels, giving rise to properties such as absorption and fluorescence.^{3–8,96}

Metal NCs represent a new class of luminescent nanomaterials with metal cores consisting of a few to tens of atoms.^{8,14,95,98,99} These NCs act as a bridge between atoms and NPs; however, they can readily coalesce to form NPs if they are not stabilized using special gas, liquid, polymers, and biomolecules.^{3,5,8,17,96,100} They possess molecule-like properties such as discrete electronic states resulting in unique and tunable optical, chemical, and electronic properties such as high quantum yield fluorescence, electrochemoluminescence (ECL), SERS, and photostability. There are many reviews on metal NCs,^{2,4–6,8,36} and a brief overview of AgNCs formed in solution is provided below; however, this review focuses on DLW-mediated AgNCs and their properties and applications.

Synthesis or Formation of AgNCs. Similar to other metallic NCs, AgNCs are subnanometer in size with a few to tens of silver atoms, and they exhibit unique properties such as strong fluorescence and photostability.^{5,8,14,24,101} Broadly speaking, AgNCs can be synthesized using bottom-up and top-down approaches.⁶ The bottom-up approach refers to atom-by-atom construction that results in ultrasmall nanomaterials with fewer defects and with homogeneous chemical

compositions. In bottom-up approaches, silver ions are reduced to zerovalent silver atoms using different reduction methods such as chemical reduction, photoreduction, electrochemical reduction, microwave reductions and sonochemical reduction.^{3,12–14,16–21,24–26,28,30,31,102–105} One of the common methods of synthesizing AgNCs is the chemical reduction method. In this method, chemical reducing agents such as sodium borohydride (NaBH₄) and sodium hypophosphite (NaPO₂H₂·H₂O) are used to reduce silver ions to AgNCs in the presence of stabilization agents.^{3,18,19,26,28,30,31,102,103} Similarly, UV and visible light have been used to reduce the silver ions to produce NCs using the photoreduction process, which has several advantages such as controlled reduction without introducing impurities.^{12–14,16,17,25,106} The method of AgNC formation by microwave-assisted reduction is simpler, faster, and highly reproducible,^{104,105} whereas the electrochemical reduction method has the advantage of producing NCs with well-defined size.^{20,21} On a similar note, sonochemical reduction is an energy efficient method and has been proven to be a useful method to produce NCs using ultrasonic irradiation.²⁴ AgNCs can also be formed by a top-down approach where silver nanoparticles (AgNPs) are etched using chemical, high temperature, etc., using techniques such as interface etching and direct core reduction of large AgNPs.⁶ DLW, a new technique for synthesizing and patterning NCs, is also a bottom-up approach of NC formation; however, this approach of fabrication can form NCs with precise spatial control in the range of a few hundred nanometers and, hence, can be coined as a directed bottom-up approach.^{33,34,38,85,107}

AgNCs Possessing Unique Optical Properties. AgNCs exhibit characteristic absorption and fluorescence features that depend on the size of the particles and encapsulating scaffolds. Because they are too small to support plasmonic behavior, the absorption spectrum is devoid of a surface plasmon peak, otherwise seen at around 400 nm in the Ag NP's absorption spectrum. However, they exhibit discrete energy transitions; hence, they possess characteristic broadband absorption features due to multidisperse particles.^{3,8,108} AgNCs typically possess fluorescence with a quantum yield of several orders of magnitude higher than those of bulk metals. The enhanced optical properties are associated with the energy gap between the highest occupied and lowest unoccupied molecular orbitals that can be tuned by varying with the size and composition of NCs.^{5,8,96} The gap can also be affected by different factors like the encapsulating environment, ligands or surfactant, or concentration of chemicals. However, at present, working with AgNCs remains challenging because of its highly oxidative nature.^{3,8,96}

SERS, Solvatochromic, and ECL. AgNCs are reported to enhance the Raman signal by interacting with the analytes using a charge-transfer mechanism by the process known as SERS.^{26,109,110} For instance, an atomically precise thiolated AgNC (Ag₁₅₂) is reported to enhance the Raman signal of surrounding analytes.⁹⁵ Similarly, Dickson et al. have shown that the few-atom AgNCs produce scaffold-specific single-molecule Stokes and anti-Stokes Raman scattering.¹¹⁰ Next, AgNCs show a solvatochromic effect, which is changes in the optical and fluorescence properties due to changes in the surrounding matrixes such as changes in the solvent polarity or pH value.^{17,25} It is shown in one study by Ras et al. that when the solvent is changed from water to methanol, the absorption and emission maxima obtained from AgNCs formed in poly(methacrylic acid) (PMAA) shifted significantly toward

Table 1. Summary of NC Formation: Listings of Synthetic Strategy, Reduction and Stabilization, Nuclearity of the Silver Atom, Optical Properties, and Their Applications^a

method	encapsulation/stabilization agents	nuclearity of AgNCs	absorption/emission/quantum yield	potential applications
bottom-up, photoreduction	polymer (PMAA) ^{17,106}	(Ag ₂ , Ag ₅ , Ag ₇) ¹⁷	Abs, 530 nm/Em, 626 nm for an Ag/MAA ratio of 200%/QY, 5–6% (relative to rhodamine 101 in ethanol) ¹⁷	sensing, imaging, optical data storage, biological label ^{17,25}
bottom-up, photoreduction	dendrimer (PAMAM) ¹²	(Ag ₂ –Ag ₈) ¹²	Abs, 345 and 430 nm/Em, 533, 553, 589, 611, and 648 nm ¹²	biological label for single-molecule studies, imaging ¹²
bottom-up, photoreduction	microgel [poly(NIPAM-AA-HEA)] ²⁵	(Ag _n ⁺ , n = 4–9) ²⁵	Abs, varying from 350 to 600 nm with a light dose/Em, ~600 nm ²⁵	drug delivery, fabrication of photonic crystal, sensing ²⁵
bottom-up, photoreduction	oxides (silver oxide) ¹⁴	(Ag ₂ –Ag ₈) ¹⁴	Em, 450–480 and 510–550 nm upon excitation using light of wavelength shorter than 520 nm ¹⁴	SERS, data storage, single-molecule detection ¹⁴
bottom-up, photoreduction	amyloid fiber together with thioflavin ¹³		Abs, dominant peak at 400 nm and shoulder at 520 nm/Em, 450 nm ¹³	biological assays, cell imaging, studies of single molecules ¹³
bottom-up, photoreduction	hydrogel polyglycerol- <i>block</i> -poly(acrylic acid) ¹⁶	(Ag ₂ –Ag ₈) ¹⁶	Abs, shifting from 500 to 580 nm with increasing light dose/Em, 600 nm with a shoulder at 700 nm ¹⁶	fluorescent imaging, biomarkers ¹⁶
bottom-up, sonochemical reduction	polymer (PMAA) ²⁴		Abs, 440–520 nm depending on the light dose/Em, 610 nm upon excitation with 510 nm/QY, 11% (relative to Rhodamine B in ethanol) ²⁴	bioimaging, chemical and biosensing, single-molecule studies, and possibly catalysis ²⁴
bottom-up, chemical reduction	polymer (PEG, molecular hydrogel) ¹²⁷		Abs, peaks at 330, 426, 496 nm/Em, ~670 nm/QY, 12% with respect to DCM dye ¹²⁷	biological applications such as imaging and sensing, biomarkers ¹²⁷
bottom-up, chemical reduction	thiols (DCTB, ²⁶ phenylethanthiol, ¹⁰² DMSA) ³¹	Ag _{15,2} ¹⁰²	Abs, 460 nm/Em, peaks at 407, 425, 460, 490, and 800 nm when excited with 375 nm ¹⁰²	electronics, optics, biomedicine, ¹⁰² catalysis, sensing, ³¹ SERS substrate ²⁶
bottom-up, chemical reduction	DNA (single-stranded DNA) ^{3,8,30}	Ag ₇ ³¹ (Ag ₅ –Ag ₁₁) ³	Abs, 450 nm ³¹ Em, 523, 562, 590, 615, 635, and 670 nm depending on the DNA template ³	catalysis, spectroscopy, imaging, sensing ³ micropatterning ¹⁸
bottom-up, chemical reduction	protein (bovine serum albumin) ^{9,28,103}	Ag ₁₃ ¹⁹	Em, 647 nm for excitation of 572 nm and 573 nm for excitation of 509 nm depending on the base sequence of DNA ¹⁸	biosensing, drug delivery ¹⁹
bottom-up, chemical reduction	synthetic peptides ¹¹²	Ag ₁₅ ²⁸	Abs, 270 nm/Em, broadband 550–750 nm with peak at 670 nm ¹⁹	biolabeling and imaging ²⁸
bottom-up, chemical reduction	selenolate ¹²⁹	Ag ₇ –Ag ₁₂ ¹¹²	Abs, five intense bands at 879, 681, 574, 516, and 440 nm along with three broad bands centered at 970, 635, and 395 nm ¹²⁹	biomarker, imaging ¹¹²
bottom-up, chemical reduction	microemulsion (water-in-oil) ²⁷	Ag ₄ ¹²⁹	Abs, bands at 220–230, 250–270, and 400–450 nm/Em, 350 nm upon excitation at 290 or 270 nm ²⁷	applicable as sensors (fluorescent, magnetic, or chemical), catalysis ²⁷
bottom-up, electrochemical reduction	dodecanethiol/tetrabutylammonium ²⁰	Ag ₄ (n ≤ 10) ²⁷	Abs, band at 260, 310, and 375 nm/Em, 400 and 420 nm excitation at 325 and 350 nm, respectively ²⁰	biosensors, catalytic applications ²⁰
bottom-up, electrochemical reduction	glycine ³¹	(Ag ₅ , Ag ₆) ²⁰	Abs, 449 nm/ECL Em, 422 nm ²¹	bioanalysis ²¹
bottom-up, microwave reduction	polymer (PMAA) ¹⁰⁴		Abs-508 nm/Em-608 nm ¹⁰⁴	bioimaging, chemical, and single-molecule studies ¹⁰⁴
bottom-up, microwave reduction	glycopolymer [poly(MAA-co-MAG)] ¹⁰⁵		Abs, 520 nm/Em, 615 nm ¹⁰⁵	biological applications for both cancer imaging and targeted cancer therapy ¹⁰⁵
bottom-up, microwave reduction	glutathione ^{130–132}	Ag ₂₅ ¹³²	Abs, 340 nm/Em, 450 nm; ¹³⁰ Abs, peak start at 500 nm and shoulder at 400 nm/Em, 615 nm/QY, 7.7% (relative to quinine sulfate); ¹³² for a Ag/Au ratio of 0.2, Abs., 350, 420, and 478 nm/Em, 670 nm ¹³¹	chiral recognition and applications in biochemistry, ¹³⁰ sensing, ¹³¹ useful in biological applications ¹³²

Table 1. continued

method	encapsulation/stabilization agents	nuclearity of AgNCs (Ag ⁰ , Ag ⁺ , Ag ²⁺) ^{133,134}	absorption/emission/quantum yield	potential applications
bottom-up, radiolytic reduction	poly(phosphate) ^{133,134}	(Ag ⁰ , Ag ⁺ , Ag ²⁺) ^{133,134}	Abs, band 300–500 nm, several absorption peaks depending upon the irradiation time ^{133,134}	redox chemistry ^{133,134}
bottom-up, radiolytic reduction	sodium polyacrylate or partly carboxylated polyacrylamide or glutaric acid ²³	most probable Ag ⁺ ²³	Abs, band 250–600 nm; the 310 and 345 nm absorption peaks correspond to Ag ₇ ²³	
top-down, synthetic strategy: from NP etching, high-temperature nucleation and growth, interfacial synthesis using etching	mercaptoposuccinic acid ¹³⁵	Ag ₃₈ ¹³⁵	Abs, below 600 nm/Em, 720 nm when excited with 450 nm/QY, 0.6% (with respect to Rhodamine 6G) ¹³⁵	
top-down, synthetic strategy: from NP etching, high-temperature nucleation and growth, interfacial synthesis using etching	mercaptoposuccinic acid ¹²⁸	Ag ₇ , Ag ₈ ¹²⁸	Abs, 550 nm (for Ag ₆), no distinguishable feature in the visible region (for Ag ₇)/Em, 650 nm with 550 nm excitation (for Ag ₆) and 440 nm with 350 nm excitation (for Ag ₇) ¹²⁸	
DLW, synthesis strategy: laser reduction	glass ^{34,35,39,85–88,93,94,127,136}	Ag _m ³⁴ (m < 10) ^{34,38,39,85–88,93,94,127,136}	Abs, between 280 and 410 nm/Em, 640 nm and shoulders at 500 and 590 nm depending upon the laser dose (reported for FPL glass) ³⁸	recording/reading data, optical devices, volume holography, frequency converter, glass fibers, etc.
DLW, synthesis strategy: laser reduction	zeolites ^{32,37,42,43,89,137}	Ag _m ³⁴ , where m < 10 ^{37,42,43,89}	Em, 540 nm upon 375 nm excitation (reported for silver exchange Zeolite 3A) ³⁷	QR codes, fluorescent light source, organic LED, data storage ^{32,37,42,43,89}
DLW, synthesis strategy: laser reduction	polymers ^{33,90–92}		Abs, 435 nm/Em, 500–750 nm with a maximum at 560 nm ^{33,90–92}	imaging, data storage, microlabel, SERS substrate ^{33,90–92}

^aAgNCs are represented by Ag_m³⁴, where m is the nuclearity and x+ is the ionization degree. Some cells of the table are left blank because relevant information was not found. Acronyms used: Abs, absorption; Em, emission; QY, quantum yield; PMAA, poly(methacrylic acid); PAMAM, poly(amidoamine); poly(NIPAM-AA-HEA), poly(N-isopropylacrylamide-acrylic acid-2-hydroxyethyl acrylate); PEG, poly(ethylene glycol), DCTB, *trans*-2-[3-(4-*tert*-butylphenyl)-2-methyl-2-propenylidene] malonitrile; DMSA, *meso*-2,3-dimercaptosuccinic acid; DNA, deoxyribonucleic acid; MAG, 2-(methacrylamido)glucopyranose; MAA, methacrylic acid.

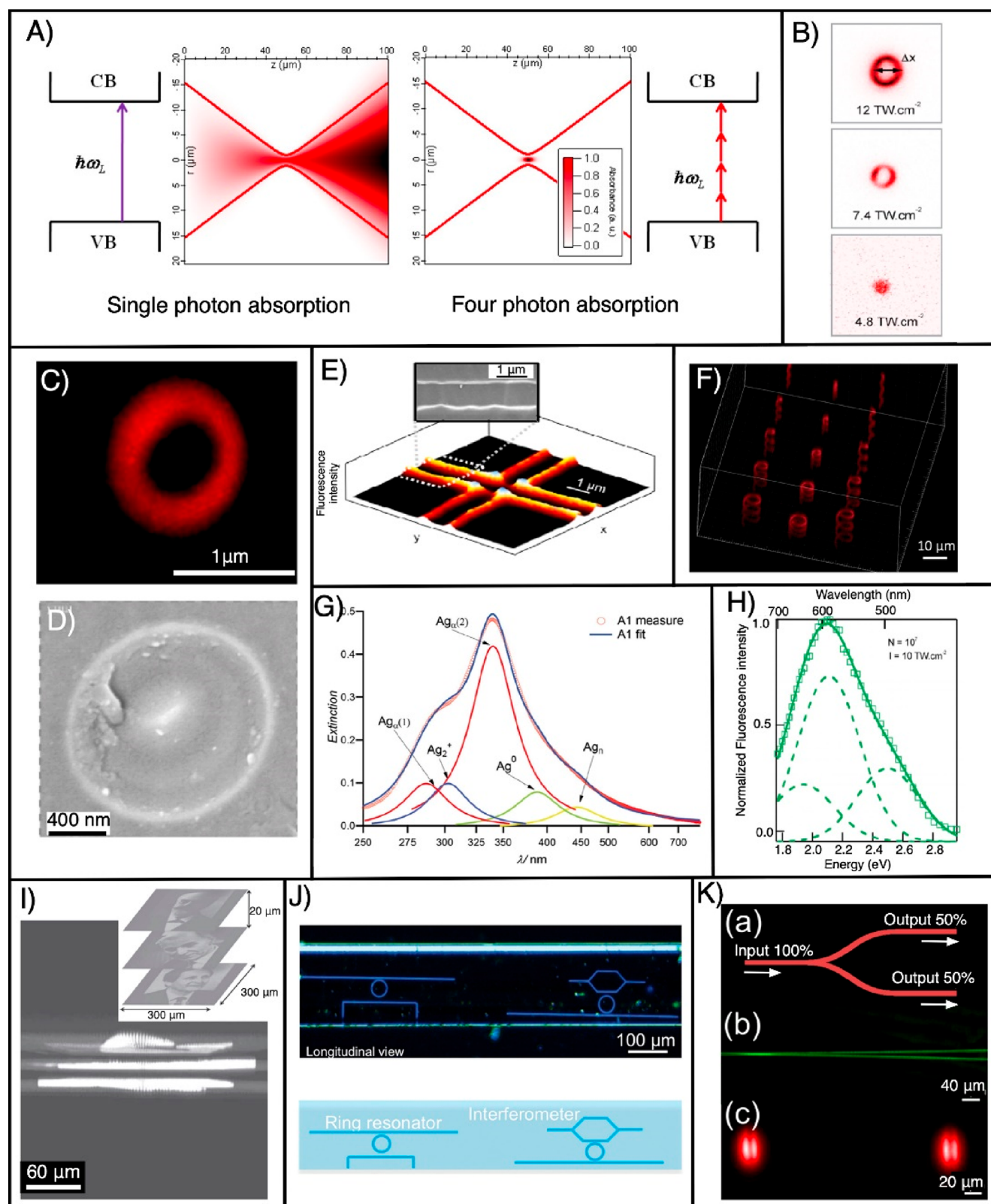


Figure 3. (A) Illustration of single- and four-photon absorption of a Gaussian beam focused with an objective lens of numerical aperture 0.5. Because of four-photon absorption, the laser energy is absorbed within the focal volume inside the glass containing silver and results in the formation of AgNCs@glass precisely in 3D space. Reproduced from ref 40. Copyright 2009 Optical Society of America. (B) Fluorescence images (excitation wavelength = 405 nm) of the laser-written ring-shaped structures at three different irradiances. Reproduced from ref 38. Copyright 2010 American Chemical Society. (C) Fluorescence confocal microscopy image of a photoinduced ring structure when excited with a 405 nm laser (fabrication parameters: wavelength = 1030 nm, repetition rate = 1 MHz, NA = 0.52, and deposited energy = 166 nJ). Reproduced from ref 93. Copyright 2010 Elsevier. (D) Corresponding high-resolution scanning electron microscopy (HRSEM) image. Reproduced from ref 38. Copyright 2010 American Chemical Society. (E) Fluorescence and HRSEM images (inset) of a AgNC containing a 2D pattern. Reproduced from ref 85.

Figure 3. continued

Copyright 2009 Optical Society of America. (F) 3D pattern created inside the glass by DLW. (G) Extinction spectrum of AgNCs@glass. Reproduced from ref 145. Copyright 2014 John Wiley and Sons. (H) Normalized fluorescence spectra of laser-written NCs with a laser wavelength of 1030 nm, an irradiance of $10 \text{ TW}\cdot\text{cm}^{-2}$, and 10^7 pulses at a repetition rate of 10 MHz. Reproduced from ref 38. Copyright 2010 American Chemical Society. (I) Confocal fluorescence images (excitation wavelength = 405 nm) of three French Nobel Laureates in physics [Gabriel Lippmann (1908), Alfred Kastler (1966), and Claude Cohen-Tannoudji (1997)] patterned on top of each other using DLW of AgNCs@glass. Reproduced from ref 39. Copyright 2010 John Wiley and Sons. (J) Ring resonator and Mach–Zehnder interferometer written in silver-containing glass ribbon fibers. Reproduced from ref 146. Copyright 2015 John Wiley and Sons. (K) Beamsplitter (50–50) fabricated inside the silver-containing glass. Reproduced from ref 136. Copyright 201 Springer Nature.

the red.¹⁷ A solvatochromic effect was also seen in AgNCs stabilized in DNA oligonucleotides.¹¹¹ In addition to photoluminescence, AgNCs also exhibit ECL. ECL is an emission of light stimulated by electricity in an appropriate chemical environment.^{17,32} This is reported in AgNCs by Ras and co-workers, and they have demonstrated cathodic hot electron-induced ECL properties of AgNCs.¹⁷

Broad Range of Applications. Because of the unique properties of AgNCs, they have already been utilized in several applications such as imaging, sensing, data storage, and labeling.^{4,6,8,100,112} They are very small materials and mostly biocompatible and exhibit bright fluorescence; therefore, NCs have been used for fluorescence imaging of cancer cells,^{113,114} amyloid fibers,¹³ living cells, and even the nuclei of cells.¹¹⁵ They have also been used to detect some of the metal ions such as copper, chromium, and mercury.^{116–118} Detection is mainly based on the fluorescence quenching of AgNCs and they are used to detect these metal ions with a concentration in the nanomolar range.¹¹⁹ Further, AgNCs are also able to detect biomolecules, proteins, DNA, and RNA.^{120–125} They are also used for data storage in silver oxide thin films, glass, and zeolites and have been utilized for the fabrication of microlabels in zeolites and polymers.^{38,42,85} Some AgNCs exhibit nonlinear-optical properties such as second or third harmonic generation and have been utilized to write and read data.^{34,126}

To provide readers with an overview of the AgNCs, we summarize the various synthesis strategies, nuclearity (number of central metal atoms in a coordination compound), optical properties, and potential applications of AgNCs fabricated using different techniques including DLW in Table 1 of this review.

Commonly used solution-based synthesis methods are good at producing AgNCs in large amounts; however, they cannot provide control over NC formation at the specific spatial locations; this is necessary for the fabrication of solid-state monolithic functional devices such as SERS substrates and thin-film nanosensors. Laser-written AgNCs, synthesized through photoreduction on a solid-state substrate, have several advantages over the solution-based AgNCs. One of the advantages is precise spatial control of NC formation at a resolution of sub-500 nm. Solution-dispersed fluorescent AgNCs are, in general, photostable; however, they cannot match the photostability of laser-written AgNCs in a solid-state substrate (especially in a glass substrate). Further, the precise use of a laser dose within a precision of a few hundred nanometers allows efficient control of the nucleation and growth of AgNCs, which enables a systematic study of growth kinetics and changes in the NC properties during its formation. Laser-written AgNCs have been realized in a solid-state substrate, namely, glass, zeolites, and polymers, by a few groups, as described in the next section.^{33,37,38,42,85,90,136,137}

4. DLW of AgNCs in Glass

Glass is the most common stabilizing scaffold/substrate for generating NCs using DLW.^{34,38,40,85} The process of generating AgNCs using DLW in glass (AgNCs@glass) can be divided into two steps: (i) preparation of silver-ion-laden glass and (ii) activation of NCs by reducing silver ions.^{38,138} AgNCs@glass are generated (activated) by irradiation of the silver-ion-laden glass by a focused-laser beam^{38,39,139} γ irradiation,¹⁴⁰ electric-field-assisted diffusion (EFAD) and successive annealing,¹⁴¹ and thermoassisted stabilization.⁸⁶

There are reports of a few silver-laden glasses such as sodalime glass, oxyfluoride, and phosphates glasses that can generate AgNPs and AgNCs.¹⁴² Femtophotoluminescent (FPL) glass is a perfect example because the AgNCs formed inside this glass are highly emissive and exceptionally photostable. This glass is prepared by a standard glass melting technique, where the raw materials are $(\text{NH}_4)_2\text{HPO}_4$, ZnO, AgNO_3 , and Ga_2O_3 powder.³⁸ In FPL glass with composition $40\text{P}_2\text{O}_5\text{-}4\text{AG}_2\text{O-}55\text{ZnO-}1\text{Ga}_2\text{O}_3$ (mol %), ZnO- P_2O_5 forms a network, Ag_2O is the silver source for NC formation, and Ga_2O_3 enhances the stability of the glass matrix. This glass is visibly transparent and exhibits an absorption cutoff at around 280 nm due to silver-ion-associated absorption. This glass displays an excitation band at 265 nm and an emission band at 380 nm with the dipolar transition $4d^{10} \rightarrow 4g^5s^1$ of the isolated Ag^+ ions. A weak emission is also observed at 520 nm, which corresponds to $\text{Ag}^+\text{-Ag}^+$ pairs in a small amount.^{38,85}

DLW instrument equipped with a femtosecond laser source emitting an average laser beam of power of 5 W with 470 fs, a 10 MHz repetition rate at 1030 nm wavelength was used to write AgNCs@glass in a pipe-shaped fluorescent 3D structure within FPL glass.³⁸ (Figure 3A–H). The nonlinear absorption of light creates a submicron voxel allowing for patterning of 3D fluorescent structures inside the glass. The irradiated sample presents a weak absorption between 280 and 410 nm, which corresponds to the absorption peak of photoinduced NCs.

The emission spectra obtained from the as-formed AgNCs@glass is broadband; however, the shape and position of the peak is dependent on both irradiance and the number of pulses. At low irradiance, a band with a maximum at 640 nm and a shoulder with a maximum at 500 nm are obtained. With an increase in the irradiance, the band at 640 nm decreases considerably and the band with a peak at 500 nm slightly increases, while a new band with a maximum at 590 nm appears. However, a further increase in the irradiance drastically decreases the band with a maximum at 640 nm compared to that of two other bands. Hence, by adjustment of the dose, the emission can be tuned from red to yellow.³⁸

The fluorescence intensity of AgNCs@glass is also strongly influenced by the laser repetition rates, irradiation, and number of pulses. A high repetition rate of the writing beam is directly proportional to the fluorescent intensity and results in thermal

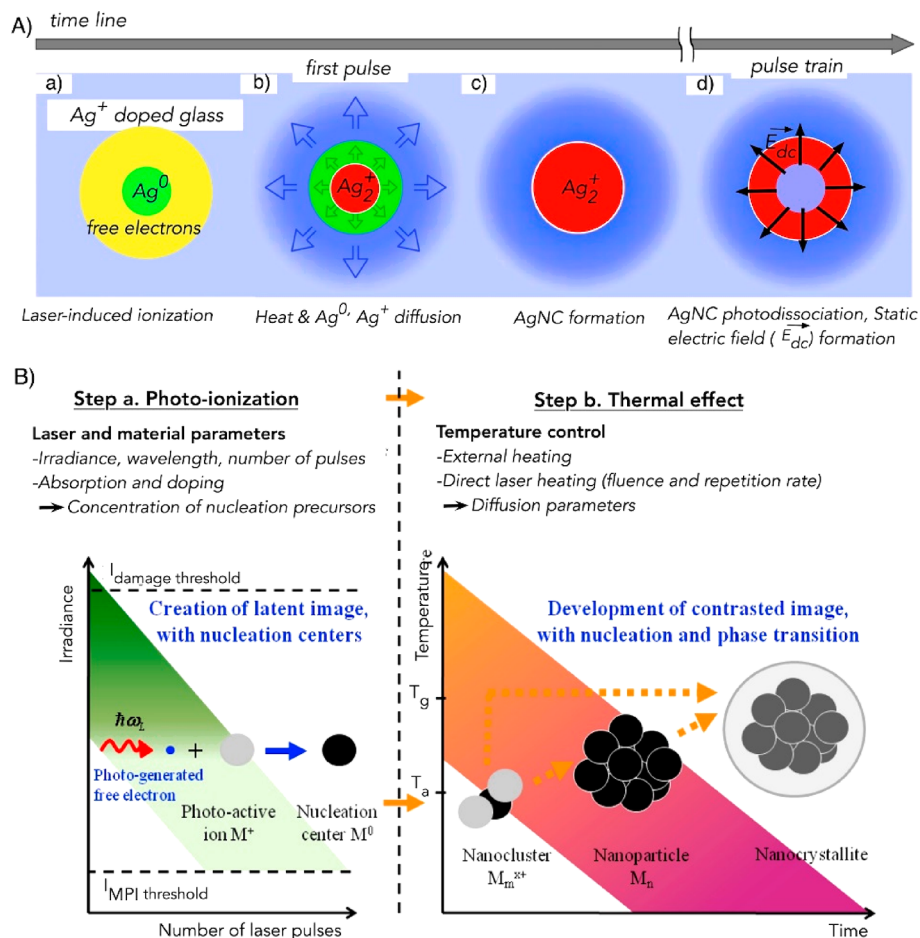


Figure 4. Formation mechanism of AgNCs@glass. (A) Diagram depicting the physical phenomena occurring during laser-induced AgNCs@glass formation. Reproduced from ref 147. Copyright 2016 American Physical Society. (B) Diagram portraying the processes of formation of NCs, NPs, and nanocrystallites. After formation of the nucleation center due to photoionization, NCs grow to form NPs and nanocrystallites with an increase in thermal treatment. T_a and T_g are the activation and glass transition temperatures, respectively. MPI is multiphoton ionization. Reproduced from ref 40. Copyright 2009 Optical Society of America.

diffusion, causing silver atoms and ions to diffuse and aggregate into AgNCs. The combined effect of thermal diffusion, photodiffusion, and photodissociation leads to localization and stabilization of NCs in the border of the irradiation zones (Figure 3C–F). Further, both irradiance and the number of pulses affect the fluorescence, the former linearly and the latter logarithmically.³⁸

AgNCs@glass exhibits nonlinear-optical properties such as second and third harmonic generation. The fluorescence and second-harmonic-generation correlative microscopy study demonstrates that during laser writing inside the silver-doped glass substrates, a laser-induced frozen charge gradient results in a permanent and stable electric field buried inside the modified glass. This gives rise to a second-order nonlinearity by the well-known electric-field-induced second-harmonic-generation effect.^{94,126,143,144} Further, AgNCs formed by direct laser irradiation in silver-containing zinc phosphate glass exhibit a third-harmonic-generation signal due to the change in the third-order susceptibility, and this signal is used for data storage.³⁴

Mechanisms of AgNCs@glass Formation. Upon laser exposure, a nonlinear four-photon interaction ejects free electrons from the valence band to the conduction band of the glass (Figures 3A and 4A,B).^{38,85,93} The released electron reduces silver ions and forms zerovalent silver (Ag^0), which

aggregates with the silver ion to form Ag_2^+ , and this is followed by a chain reaction to produce Ag_m^{x+} , which is an emissive silver species.^{38,145} Furthermore, the high laser repetition rate accumulates thermal energy and increases the local temperature, which causes diffusion of the silver species (Figure 4A,B).^{40,85,147} Mobile Ag^0 atoms are trapped by the Ag^+ ions to form silver clusters Ag_m^{x+} ($m < 10$ is the number of atoms and x is the ionization degree). Subsequent exposure interacts with newly created AgNCs and leads to photodissociation in the center of the laser beam. This results in the formation of a ring-shaped structure at the periphery (Figure 4B).^{38,40,85,147} The creation of emissive silver species upon laser irradiation enables writing of a 3D structure within the glass substrates (Figures 3E,F and 4).³⁹ The laser writing produces a pipeline structure along the propagation constant axis with a wall thickness of 80 nm.^{38,85}

Additionally, several efforts have been made to further understand the mechanism, the distribution of silver species, and the glass network structure in a silver-laden glass matrix.^{93,143,147–149} For instance, in one study, Bourhis et al. investigated the excitation mechanism in AgNC@glass formation using a transient absorption pump–probe experiment and found that the four-photon-absorption mechanism was involved for the photoexcitation process.⁹³ A correlative study that included near-field scanning optical microscopy,

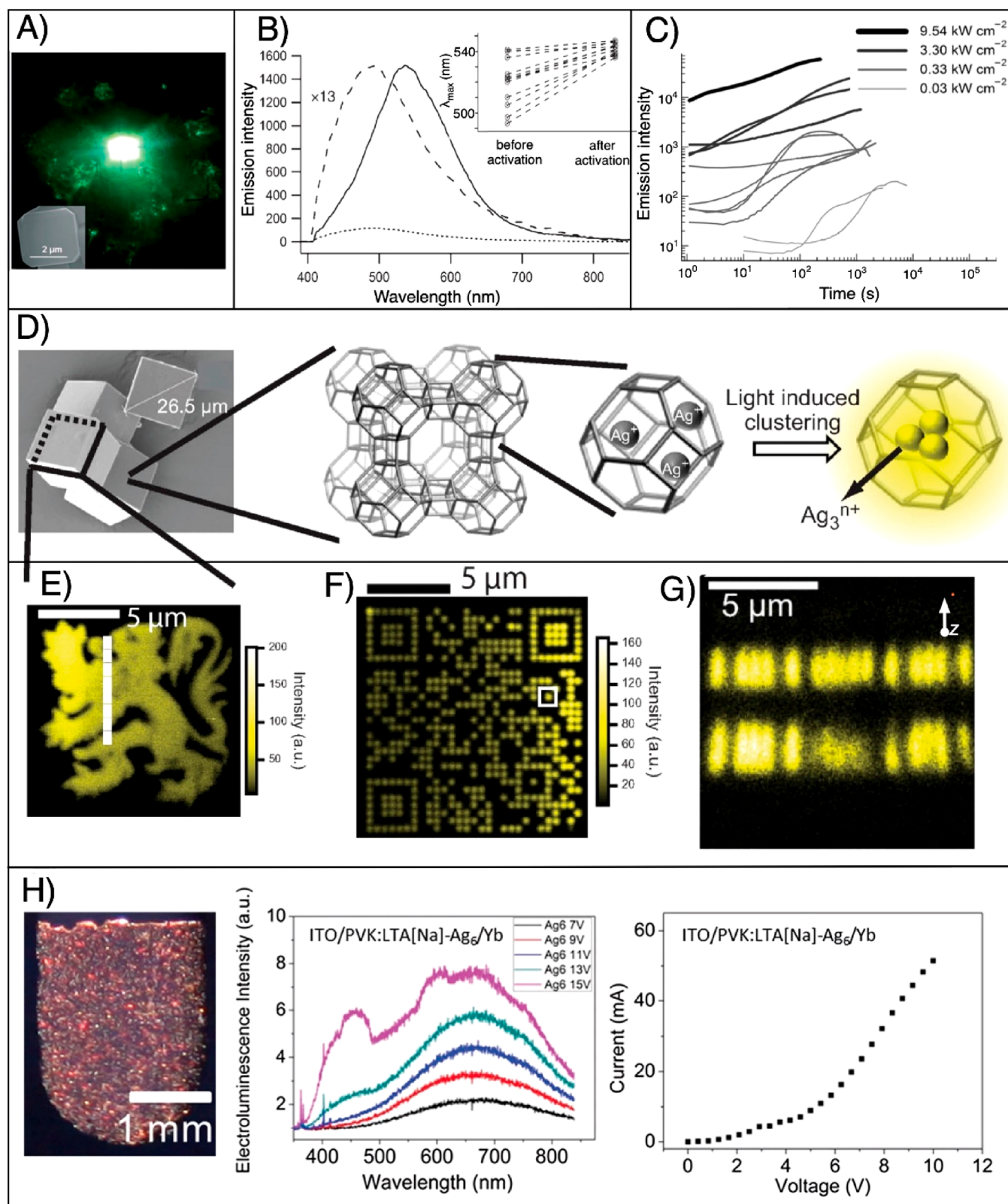


Figure 5. Laser-based formation and patterning of AgNCs@zeolites. (A) True-color fluorescence image taken of the green emission from AgNCs@zeolites and inset showing the SEM image of a characteristic silver-exchanged zeolite A crystal. Reproduced from ref 137. Copyright 2008 John Wiley and Sons. (B) Emission spectrum before (small dashed line) and after (solid dashed line) photoactivation of an individual silver-laden zeolite crystal. The normalized spectrum before activation is amplified 13 times (big dashed line). The inset shows emission maxima before and after photoactivation for 11 individual crystals. Reproduced from ref 137. Copyright 2008 John Wiley and Sons. (C) Time evolution of the emission intensity of 11 different individual silver-containing zeolite crystals excited with four different activation intensities. Reproduced from ref 137. Copyright 2008 John Wiley and Sons. (D) Schematic showing the photoactivation process of AgNCs@zeolites. From left to right: HRSEM image of a zeolite crystal, multiple cage structure of zeolite crystals, and single-crystal structure of zeolites with embedded silver ions, followed by the light-

Figure 5. continued

induced activation of AgNCs@zeolites. (E) Fluorescence microscopy image of a heraldic lion fabricated using two-photon DLW inside a silver-laden zeolite single crystal. Reproduced from ref 42. Copyright 2010 John Wiley and Sons. (F) Fluorescence image of the QR code encoded with “Katholieke Universiteit Leuven” by two-photon DLW. Reproduced from ref 42. Copyright 2010 John Wiley and Sons. (G) Fluorescence image showing the writing of different 2D QR codes on top of each other. Reproduced from ref 42. Copyright 2010 John Wiley and Sons. (H) AgNCs@zeolite-based LED light source. From left to right: Composite LED [10 wt % (LTA-type zeolites + AgNCs) + poly(vinyl carbazole)], ECL spectra at different voltages, and current–voltage curve. Here Na is sodium, ITO is indium–tin oxide, and Yb is ytterbium. Reproduced from ref 32. Copyright 2017 John Wiley and Sons.

chemical microprobe analysis, numerical modeling, and spatial profiling after soft etching has been reported, and this study elucidated the laser-induced silver redistributions (ions, clusters, and hole centers) in a silver-containing phosphate glass.¹⁴⁹ Another correlative study that included fluorescence and second-harmonic-generation microscopy revealed that the generated electric field due to distribution of the NCs was a key factor for silver clustering and the formation and stabilization of AgNCs@glass required favorable reduction–oxidation conditions.¹⁴³ However, all of these studies are not able to fully elucidate the mechanisms behind NC formation, their enhanced properties, and the effect of the stabilization matrix on the NC properties.

Applications of AgNCs@glass. DLW of AgNCs@glass has already been utilized for many applications. One of them is the long-term high-capacity optical recording medium lasting for centuries; otherwise, the recording medium available today suffers from a limited lifetime (~5–10 years).³⁹ As a proof-of-concept of long-term 3D data storage, 100 × 100 pixel images of three French Nobel Laureates were encoded and patterned over one another inside a silver-containing glass substrate (Figure 3I). These structures can withstand annealed processes from 100 to 350 °C for 3 h compared to the current standard for data storage of 80 °C.³⁹ Laser-written AgNCs@glass have also been used for the fabrication of super-resolved nanostructures, optical grating, optical switching, micro-polarizer, filter, ring resonator, and interferometer (Figure 3J), display, optical recording/erasing, waveguide, volume holography, frequency converter, and photowritable glass fibers (Figure 3K).^{40,41,136,146,150,151} The fabricated structures are highly stable and show outstanding tolerance against temperature, aging, and humidity.^{38,39,85,152} Structures show superior photostability because they do not lose fluorescence even after continuous irradiation of blue light (intensity 100 kW/cm²) for hours.

5. DLW of AgNCs in Zeolites

Zeolites, also called molecular sieves, are crystalline solid structures made of silicon, aluminum, and oxygen, forming a framework of pores and channels. Small molecules, water, and cations such as Ag⁺, Na⁺, K⁺, Ca²⁺, and Mg²⁺ can reside within these pores. Zeolites have been used as encapsulating scaffolds for forming AgNCs. In the formation process, silver ions are reduced by a chemical reductant (hydrogen gas or sodium borohydride) or by γ and visible-light irradiation, whereas the zeolite cages prevent their aggregation into larger NPs.^{37,43,107,153,154}

Emissive AgNCs are formed within the framework of the zeolite due to a photoreduction process using a UV laser (Figure 5A).¹⁰⁷ The laser-generated AgNCs in zeolites (AgNCs@zeolites) emit fluorescence of wavelength ranging from 400 to 800 nm with a maximum at 540 ± 40 nm when excited with 375 nm (Figure 5B,C). Further, zeolite crystals

treated thermally are 10 times more fluorescent compared to untreated crystals. Enhanced emission occurs for the following two reasons. The first is the formation of charge-transfer complexes between partially dehydrated silver ions and oxygen atoms in zeolites. The second is the self-reduced NCs upon heat treatment.¹⁰⁷ The AgNCs@zeolites do not blink, unlike quantum dots, which are limited in many applications due to photoluminescence intermittency.¹⁰⁷

NC activation using a focused-laser beam resulted in diffraction-limited bright spots at specific domains inside an individual crystal (Figure 5D–G).⁴² Both single- and two-photon laser writing are reported to generate AgNCs@zeolites and thereby can write fluorescent structures. The resolution of writing is diffraction-limited, where the lateral resolution for single-photon writing with a laser beam of 390 nm focused with an objective lens (oil immersion, NA = 1.3) is 600 nm and the axial resolution is 4.3 μ m. For two-photon DLW performed with a laser beam of wavelength 790 nm focused with the same objective lens, the lateral resolution is estimated to be 249 nm and the axial resolution is around 1 μ m. In effect, the laser spot was scanned in three dimensions to write different structures such as heraldic lion and Quick Response (QR) codes, etc., as shown in Figure 5E–G.⁴²

Mechanism of AgNCs@zeolites Using Laser Reduction. Silver ions are reduced by light, and the reduced silver particles coalesce to increase the nuclearity; however, the molecular dimension of the zeolite cage confines the growth and prevents aggregation into larger NPs. The dynamics of the activation process of AgNCs@zeolites is studied by continuously recording emission spectra during NC formation (Figure 5C).¹³⁷ A plot of the emission intensity as a function of time shows a lag time of a few hundred seconds before actual activation by UV light. This suggests that AgNCs@zeolites need to acquire a minimal nuclearity for high fluorescence. After continuous irradiation, the emission intensity reaches a maximum, signifying the formation of AgNCs@zeolites, and shows plateau behavior, suggesting the creation and destruction of the NCs. However, prolonged exposure results in the formation of larger nonfluorescent AgNPs. There is heterogeneity in the activation curve, which is due to heterogeneity inside a zeolite crystal or between individual crystals in a population. Luminescence time decay, studied using single-photon-counting experiments, revealed that AgNCs@zeolites show three different decay times of approximately 100 ps, 1 ns, and 4 ns, which are attributed to different nuclearities of the emissive AgNCs.^{107,154}

Applications of Laser-Written AgNCs@zeolites. The photoactivated AgNCs@zeolites are reported for several applications such as data storage and fluorescent light source.^{8,32,42} Two-photon DLW allows for the fabrication of a AgNCs@zeolites microstructure within different *z* planes of the zeolite crystal (Figure 5G).⁴² Shown in the figure (only side view) are two different QR codes (similar to the QR code

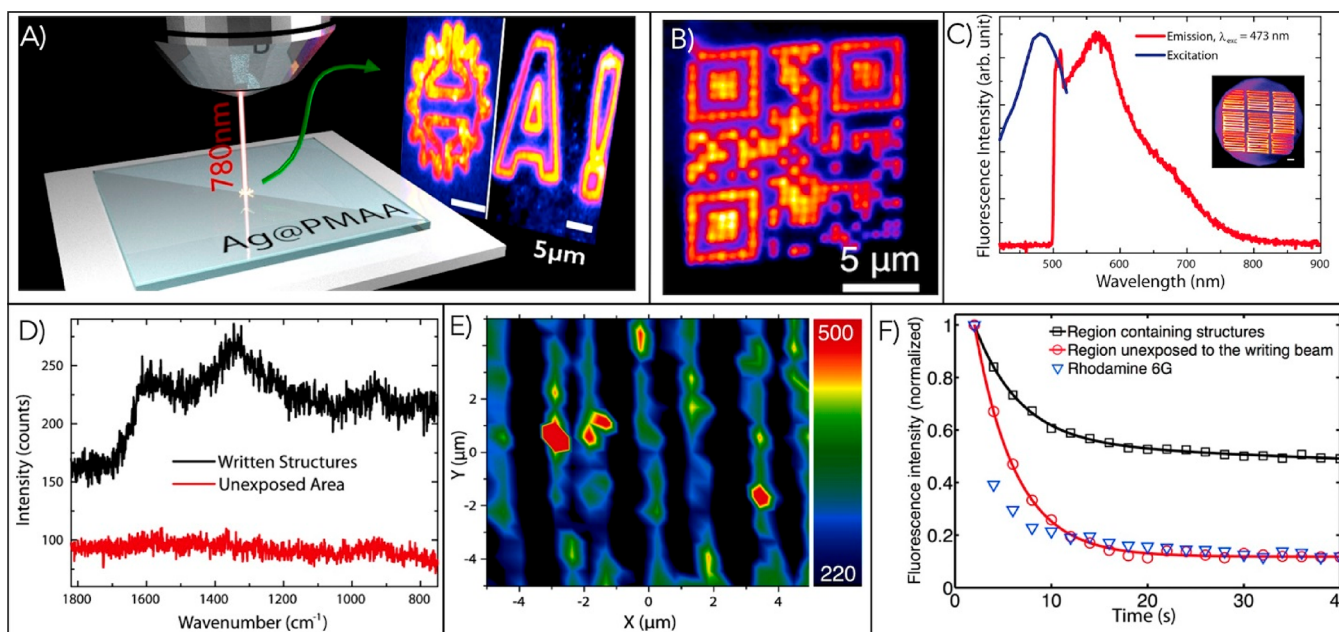


Figure 6. (A) Multiphoton DLW of AgNCs in PMAA polymer. Reproduced from ref 33. Copyright 2014 American Chemical Society. (B) Fluorescence microscopy image of a microlabel (QR code) comprised of AgNCs@polymer patterned using single-photon DLW. Reproduced from ref 90. Copyright 2016 Springer Nature. (C) Emission and excitation spectra obtained from AgNCs@polymer. The inset shows the arrays of a laser-written line comprised of AgNCs@polymer. Reproduced from ref 33. Copyright 2014 American Chemical Society. (D) Raman spectra detected from the written structures (black curve) and unexposed regions (red curve). Reproduced from ref 33. Copyright 2014 American Chemical Society. (E) Raman microscopy image of the laser-written microlines with AgNCs@polymer. (F) Comparison of the photostability of as-formed NCs with a well-known organic dye Rhodamine 6G dye and a silver-ion-containing PMAA film (not exposed to light). Reproduced from ref 33. Copyright 2014 American Chemical Society.

shown at Figure 5F) encoded with “KULeuven” and “LPS” written on top of one another within a distance of 4 μm . These two structures can be easily read without any crosstalk between the layers, and the photostability of the formed AgNCs@zeolite patterns is remarkably high compared with that of fluorescent organic dye.⁴² Because of their high fluorescence and excellent photostability, the AgNCs@zeolites can be used as a fluorescent light source.^{8,42} On that note, Kennes et al. demonstrated the fabrication of an organic LED using the electroluminescence properties of AgNCs@zeolites (Figure 5H).³² These highly fluorescent NCs as a light source are excellently stable against oxygen and humidity and exhibit a tunable wavelength; otherwise, a lot of commonly used emitters are susceptible to oxidation and humidity.³²

6. DLW of AgNCs in Polymers

Two polymers, namely, poly(methacrylic acid) (PMAA) and poly(vinyl alcohol) (PVA), have been used as scaffolds in generating AgNCs in polymer (AgNCs@polymer) using DLW.^{90–92} PMAA is a hydrophilic polymer and is extensively used as a stabilizing scaffold for encapsulating brightly fluorescent AgNCs in solutions.¹⁵⁵ PMAA is reliably used as a capping agent for generating AgNCs under different reduction processes such as photoreduction, microwave reduction, and sonochemical reduction. This polymer consists of a carboxylic acid functional group, which has a strong affinity for silver ions and silver surfaces.^{17,24,104} PMAA can also act as a OH radical scavenger that prevents the oxidation of small AgNCs.²⁴ PVA, a widely used polymer recognized as an embedding material for AgNPs, has also been demonstrated to stabilize AgNCs.⁹²

Both multiphoton- and single-photon-absorption DLW is reported to 2D pattern photostable fluorescent user-defined structures comprised of fluorescent AgNCs@polymer in PMAA polymer thin films (Figure 6A,B).^{33,90} For example, a photostable microscale fluorescent QR code is fabricated using single-photon DLW, which can be used in microlabeling applications such as authenticity marking and fluorescent tagging (Figure 6B). This structure is fabricated using very low intensity laser light of 45 GW m^{-2} , which corresponds to a laser power of 0.75 mW, and even a low-power laser pointer can deliver this amount of power.

The AgNCs@polymer structures emit fluorescence when excited with wavelengths ranging from 420 to 520 nm, and the maximum fluorescence is observed for 470 nm excitation. These structures exhibit broadband emission ranging from 500 to 750 nm with a maximum at 560 nm (Figure 6C).³³ The position and shape of the emission spectrum are characteristic of AgNCs and are similar in character to those observed in solution.^{17,33} Further, AgNCs@polymer also exhibits a SERS signal (peak at 510 nm) suggested to be generated by the charge-transfer mechanism between the polymer and NCs (Figure 6D,E).³³ The Raman spectroscopy study revealed the absence of Raman peaks in the spectrum of the area not exposed to the laser beam, whereas Raman signals are observed in the spectrum from the written structures [1590 cm^{-1} , $\nu_{\text{CO}_2^-}(\text{asym})$; 1335 cm^{-1} , $\nu_{\text{CO}_2^-}(\text{sym})$].³³ The presence of CO_2^- functional groups indicates that they are responsible for stabilization of the AgNCs. It is also reported that the photostability of AgNCs@polymer is superior to a well-known organic dye, Rhodamine 6G (Figure 6F). The high fluorescence with photostability shows that AgNCs@polymer can be an ideal replacement for organic dyes, which are often

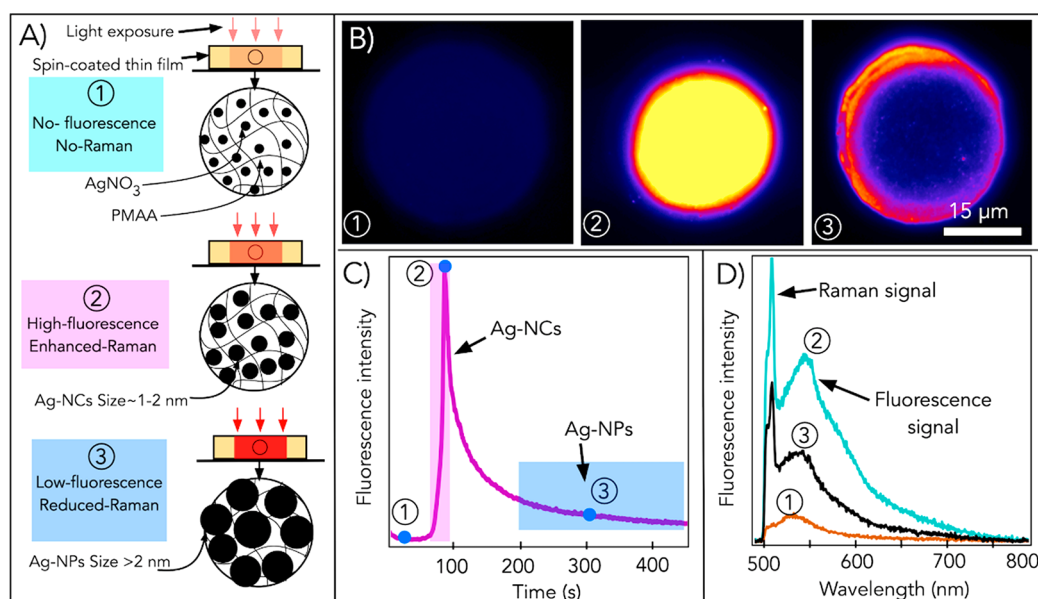


Figure 7. Formation of AgNCs in silver-containing polymer (PMAA) thin films. (A) Cartoon showing the laser-based formation of (1) silver ions, (2) AgNC or NCs, and (3) AgNPs or NPs by controlling the laser dose. (B) Fluorescence image, (C) fluorescence intensity, and (D) emission spectra for points 1–3. Reproduced from ref 90. Copyright 2016 Springer Nature.

limited by photobleaching. It is also shown that the fluorescent structures are stable and brightly fluorescent upon storage in ambient room lighting for the investigated period of 6 weeks.⁹⁰

Next, a single-exposure, submicron-scale, and arbitrary patterning of fluorescent AgNCs@polymer microstructures in a PMAA matrix is also reported.⁹¹ The technique is based on a patterning of the laser beam using a spatial light modulator (SLM). In this report, a precalculated phase pattern is encoded into the SLM that patterns the impinging laser beam, which reduces the silver ion to NCs with submicroscale spatial control. This technique precludes the use of the scanning stage, meaning a reduction in cost and a significant decrease in the fabrication time. To demonstrate the applicability of the technique, a similar photostable fluorescent microlabel like the one shown in Figure 6B is fabricated.⁹¹

PVA can also act as an encapsulating agent for the formation of AgNCs@polymer.⁹² AgNCs@polymers in PVA thin films are also found to be photostable, and they are fluorescent in the visible wavelengths. The photoluminescence property and stability of AgNCs@polymer are similar to those of laser-written AgNCs in PMAA. It is claimed in the article that PVA is an inexpensive, widely used industrial polymer with excellent features such as biocompatibility, biodegradability, and non-toxic; the technique of fabrication in this polymer thin film is cost-effective and has the potential to find numerous biology-related applications.⁹²

AgNCs@polymers have also been synthesized by laser interference lithography using a film of PMAA and silver ions.¹⁵⁶ The laser interference lithography allows a large-area patterning of the NCs at single exposure unlike DLW, which is a point-by-point scanning method of patterning. The as-formed AgNCs@polymer exhibits broadband fluorescence centered at 600 nm when excited at 488 nm. These NCs also possess a sharp peak at 510 nm, which is also suggested as an enhanced Raman scattering effect.¹⁵⁶

Formation Mechanism of Laser-Written NCs in a Polymer Thin Film. Irradiation of the laser beam to the spin-coated PMAA/silver ion film forms AgNCs.^{33,90} A 532 nm

laser beam with an intensity of 150 MW/m² is continuously irradiated to generate AgNCs in PMAA, and a series of emission spectra and intensities are recorded to study the formation mechanism of AgNCs (Figure 7).⁹⁰ On the basis of the analysis of these recorded spectra, the formation of AgNCs using DLW in the polymer is divided into three stages (Figure 7A–D). In the first stage, a quick photobleaching of a small fluorescence signal is reported, possibly a result of AgNCs kinetically trapped in PMAA yet not completely protected by the methacrylate units. This is followed by a second stage where a sharp rise in the fluorescent intensity indicating the formation of photostable NCs well protected by methacrylate units is reported. In this stage, silver ions get reduced to AgNCs, which are immediately coated by PMAA. The encapsulation process does not allow further growth of AgNCs to the formation of larger NPs, thereby stabilizing as-formed AgNCs. The third stage is marked by a slow exponential photobleaching of the fluorescence as AgNCs grow larger into nonfluorescent NPs.⁹⁰ However, these results are mostly suggestive, and more studies are needed to fully elucidate the detailed formation mechanism and enhanced properties of as-formed NCs.

Application of Laser-Written NCs in Polymers. Laser patterning of NCs in a polymer film has been shown to fabricate fluorescent microlabels that have the potential for applications like authenticity marking and fluorescence tagging.⁹⁰ This technique of NC formation is anticipated for many other applications such as imaging, superresolution imaging, cell labeling, sensing, and fluorescent tagging.^{33,90} However, to realize these applications, one needs to extract NCs from the ~40 nm polymer film without losing their special properties, which is technically challenging. Additionally, the as-formed NCs are reported to exhibit enhanced Raman signatures, and they can possibly be used as a SERS substrate.³³ Also, laser interference lithography is also reported to generate NCs in a polymer substrate, and this technique of fabrication is anticipated for the development of a biocompatible material with antifouling properties and enhanced surface

area for decreasing bacterial attachment in prosthesis and medical supplies.¹⁵⁶

Reports of Patterning of NCs of Other Metals and Encapsulating Agents. Although this review mostly focused on DLW of AgNCs, we believe the DLW method of NC formation is generic and can be used to synthesize and pattern NCs of other metallic elements. On the same note, one article presented a fast CO₂ laser patterning of spherical sub-10-nm metal NPs using laser photothermal synthesis and writing. The method was demonstrated to fabricate sub-10-nm NPs of nickel, copper, and silver directly in polymer thin films.¹⁵⁷ Another recent article reported a submicrometer writing of fluorescent gold NCs encapsulated in a PVA film with a low-power CW laser.¹⁵⁸ In one interesting study, patterning of AgNCs in an eggshell membrane using UV-lamp irradiation is reported. The egg membrane is double-layered with an interwoven fibrous structure and is comprised of cysteine-abundant proteins, which stabilize the NCs. This facile approach has potential applications in catalysis, SERS and chemical sensing, and fluorescent labeling.¹⁵⁹

7. SUMMARY, CHALLENGES, AND FUTURE OUTLOOK

Nanomaterials continue to find applications in many fields, enabling technologies in a wide variety of areas, and their applications are increasing very rapidly. One promising nanomaterial that has recently gained tremendous interest is NCs. Metallic NCs, with size of typically less than 2 nm, represent a new class of nanomaterials that can act as a bridge between isolated metal atoms and larger NPs. They have been widely studied because of their unique optical properties such as ultrahigh photostability, high and tunable emission, and ultrasmall size. AgNCs are typically synthesized in the liquid state using a bottom-up approach mostly by reducing silver salts in stabilizing solutions. However, the fabrication of functional devices that require solid monolithic substrates such as SERS substrates, thin-film sensors, and micro/nanotags is very difficult with solution-based methods of NC formation. More recently, manufacturing approaches such as ultrafast laser writing have been used to generate solid-state AgNCs, which exhibit strong fluorescence and photostability. Laser-written NCs have been proposed for various applications; however, they are mostly limited to laboratory research. Current studies are not adequate to understand the exact mechanism of formation and growth, geometries, and gifted properties of these NCs. An enhanced understanding of the laser-written NCs properties will advance their utilization.

NCs and NCs-based functional structures can be created using single-photon-absorption- and TPA-induced DLW techniques, which involve a tightly focused laser beam scanned in a photosensitive material such as polymer, glass, etc., to fabricate microstructures with subwavelength-size features. DLW is shown to form and pattern fluorescent silver NC microstructures in different inorganic/organic matrixes such as FPL glass, zeolite crystals, and polymers. In this context, researchers have used a femtosecond near-IR laser to fabricate highly fluorescent AgNC microstructures using four-photon-absorption phenomena in the inorganic FPL glasses, which provide an excellent matrix for NCs stabilization. The formation of highly fluorescent AgNCs@glass requires a high laser intensity of more than 4.8 TW/cm² and a laser repetition rate of more than 10 MHz; however, the laser-written emissive

species are highly stable and claimed to store data for many centuries.

A laser beam is also used to reduce silver ions to form brightly fluorescent AgNCs@zeolites. Zeolites are crystalline, highly porous materials with cage systems that offer localized stabilization of these NCs. During the activation by using heat treatment and TPA, silver ions reduce to form NCs that are confined in the cages of zeolites. AgNCs@zeolites are shown to be used as microlabels and a novel LED-based light source.

Further, DLW has also been used to form and pattern AgNCs@polymer. The synthesis of fluorescent AgNCs@polymer (in PMAA and PVA thin films) is reported using near-IR femtosecond ultrashort pulsed and CW lasers. AgNCs@polymer exhibits high fluorescence emission and photostability, although the underlying mechanism of formation and the reason for the enhanced properties of these NCs are not clearly known.

Each of these DLW techniques in different scaffolds has its own pros and cons. AgNCs@polymer and AgNCs@zeolites can have widespread use because of their ease in sample preparation techniques compared to that of AgNCs@glass. Further, laser reduction of silver in these scaffolds can be performed with a low-power CW laser. However, AgNCs@glass requires tedious sample preparation steps and usually a high-intensity laser, which are limited to a few research groups. From a scaffold point of view, the glass matrix provides better encapsulation compared to the zeolites and polymer scaffolds because AgNCs formed inside FPL glass are highly stable against temperature and humidity. Further, they are extremely photostable because these NCs do not photobleach. AgNCs@polymer and AgNCs@zeolites are also remarkably photostable compared to most organic dyes; however, they cannot match the photostability of AgNCs@glass.

It is difficult to print freeform user-defined structures using glass and zeolite substrates, although 3D patterning of NCs has been shown inside these substrates. NC formation in a polymer is even limited to 2D patterning because the thickness of the polymer film is a few tens of nanometers. However, in future, polymers can be potentially functionalized with proper functional groups to print 3D freeform structures because they offer greater design flexibility compared to the glass and zeolite scaffolds. From the application perspective, laser-induced AgNC formation in glass is extensively studied and has been reported for different applications such as recording/reading data, optical devices, volume holography, frequency converter, and glass fibers, whereas laser-written AgNCs@zeolites have been used for QR codes, a fluorescent light source, an organic LED, and data storage. AgNCs@polymer is reported mostly for microlabeling.

Although the first work on this topic was reported almost a decade ago, several current challenges in the field suggest that DLW of NCs is still in its infancy. At present, DLW of the NCs is mostly limited to silver metal; however, there are plenty of metals such as gold, copper, platinum, etc., that can replace silver. Consideration of the new metallic cluster will lead to the formation of NCs with new properties, functionalities, and applications. The printing of NCs is mostly limited to the fabrication of 2D or planar structures. Although 3D patterning has been shown in glass and zeolites, the fabrication of a freeform 3D NC structure is still a challenge. As mentioned earlier, polymers such as PMAA, if functionalized with the proper functional group that can undergo photo-cross-linking, could be a key for freeform 3D printing. In most cases, DLW of

NCs requires the use of a femtosecond laser, which is expensive and can limit the use of NCs in general. Hence, attention should be given to studies that highlight the use of a low-cost CW laser for generating NCs for its widespread use.

Characterization of these ultrasmall NCs is difficult and is mostly limited to optical spectroscopic tools such as absorption and emission spectroscopy. High-resolution imaging techniques such as transmission electron microscopy (TEM) would provide information about the shape, geometry, and distribution of the atoms within the NC constructs. However, TEM studies are extremely difficult because they require samples with thicknesses of less than 100 nm. One of the possible ways of performing the TEM study is to generate NCs within a TEM grid. This is most feasible with the polymer substrate, although irradiation of the beam of electrons during the TEM imaging process could perturb the ultrasmall AgNCs, leading to changes in their morphology and properties. In understanding light and material interactions, a better study of the shape and size of NCs and encapsulating agents will help to understand the enhanced properties of laser-written NCs and will further allow us to generate NCs with the desired properties. A comprehensive experimental study combined with theoretical (modeling and simulation) studies is desirable to understand the structure–property application of laser-written NCs.

Further, metal NCs formed in solutions are, in general, biocompatible. There are several reports that these NCs are synthesized in hydrogels, a biomimetic material, and has been used for the imaging of live cells. However, authors are not aware of the laser-written NCs used for any bioscience-related applications. A detailed biological study is needed to enable the use of NC substrates for cell growth, proliferation, migration, and differentiation and associated drug screening applications.

Special focus should be placed on the extraction of these laser-written AgNCs without any loss of their unique properties. The extraction will lead to many applications such as fluorophores for microscopy, which is one of the most anticipated applications of NCs because of its photostability and high quantum yield emission. Utilization of AgNCs in superresolution microscopy such as stimulated emission depletion (STED) microscopy will also be transformative. In STED microscopy, the resolution is directly proportional to the photostability of the fluorophore. Hence, the use of photostable laser-written NCs (especially in glass) could enhance the resolution of fluorescence microscopy, that has never been achieved before. Further, it is expected in the future that laser-written NCs enable the creation of next-generation systems such as substrates for SERS, anticounterfeiting codes, novel light-emitting nanodevices, intracellular drug delivery systems, molecular diagnostic devices, etc.

AUTHOR INFORMATION

Corresponding Author

Pranav Soman – Department of Chemical and Bioengineering,
Syracuse University, Syracuse, New York 13244, United States;
Email: psoman@syr.edu

Author

Puskal Kunwar – Department of Chemical and Bioengineering,
Syracuse University, Syracuse, New York 13244, United States;
 orcid.org/0000-0002-5668-6414

Complete contact information is available at:
<https://pubs.acs.org/10.1021/acsnm.0c01339>

Notes

The authors declare no competing financial interest.

ACKNOWLEDGMENTS

This work was partially supported by NIH R21GM129607 and R21AR076645 awarded to Prof. Pranav Soman.

REFERENCES

- (1) Park, Y. S.; Holmes, M. J.; Taylor, R. A. *An Introduction to Nanoparticles and Nanotechnology. Designing Hybrid Nanoparticles*; Morgan & Claypool Publishers, 2015; DOI: [10.1088/978-1-6270-5469-0ch1](https://doi.org/10.1088/978-1-6270-5469-0ch1).
- (2) Jin, R.; Zeng, C.; Zhou, M.; Chen, Y. Atomically Precise Colloidal Metal Nanoclusters and Nanoparticles: Fundamentals and Opportunities. *Chem. Rev.* **2016**, *116* (18), 10346–10413.
- (3) Petty, J. T.; Story, S. P.; Hsiang, J. C.; Dickson, R. M. DNA-Templated Molecular Silver Fluorophores. *J. Phys. Chem. Lett.* **2013**, *4* (7), 1148–1155.
- (4) Shang, L.; Dong, S.; Nienhaus, G. U. Ultra-Small Fluorescent Metal Nanoclusters: Synthesis and Biological Applications. *Nano Today* **2011**, *6* (4), 401–418.
- (5) Wilcoxon, J. P.; Abrams, B. L. Synthesis, Structure and Properties of Metal Nanoclusters. *Chem. Soc. Rev.* **2006**, *35* (11), 1162.
- (6) Mathew, A.; Pradeep, T. Noble Metal Clusters: Applications in Energy, Environment, and Biology. *Part. Part. Syst. Charact.* **2014**, *31* (10), 1017–1053.
- (7) Jena, P.; Castleman, A. W. *Introduction to Atomic Clusters*, 1st ed.; Elsevier BV, 2010; Vol. 1; DOI: [10.1016/B978-0-444-53440-8.00001-X](https://doi.org/10.1016/B978-0-444-53440-8.00001-X).
- (8) Díez, I.; Ras, R. H. A. Fluorescent Silver Nanoclusters. *Nanoscale* **2011**, *3* (5), 1963–1970.
- (9) Campbell, E. K.; Holz, M.; Gerlich, D.; Maier, J. P. Laboratory Confirmation of C60⁺ as the Carrier of Two Diffuse Interstellar Bands. *Nature* **2015**, *523* (7560), 322–323.
- (10) Dietz, T. G.; Duncan, M. A.; Powers, D. E.; Smalley, R. E. Laser Production of Supersonic Metal Cluster Beams. *J. Chem. Phys.* **1981**, *74* (11), 6511–6512.
- (11) Cathcart, N.; Mistry, P.; Makra, C.; Pietrobon, B.; Coombs, N.; Jelokhani-Niaraki, M.; Kitaev, V. Chiral Thiol-Stabilized Silver Nanoclusters with Well-Resolved Optical Transitions Synthesized by a Facile Etching Procedure in Aqueous Solutions. *Langmuir* **2009**, *25* (10), 5840–5846.
- (12) Zheng, J.; Dickson, R. M. Individual Water-Soluble Dendrimer-Encapsulated Silver Nanodot Fluorescence. *J. Am. Chem. Soc.* **2002**, *124* (47), 13982–13983.
- (13) Makarava, N.; Parfenov, A.; Baskakov, I. V. Water-Soluble Hybrid Nanoclusters with Extra Bright and Photostable Emissions: A New Tool for Biological Imaging. *Biophys. J.* **2005**, *89* (1), 572–580.
- (14) Peyser, L. A.; Peyser, L. A.; Vinson, A. E.; Bartko, A. P.; Dickson, R. M. Photoactivated Fluorescence from Individual Silver Nanoclusters. *Science* **2001**, *291* (5501), 103–106.
- (15) Díez, I.; Ras, R. H. A.; Kanyuk, M. I.; Demchenko, A. P. On Heterogeneity in Fluorescent Few-Atom Silver Nanoclusters. *Phys. Chem. Chem. Phys.* **2013**, *15* (3), 979–985.
- (16) Shen, Z.; Duan, H.; Frey, H. Water-Soluble Fluorescent Ag Nanoclusters Obtained from Multiarm Star Poly(Acrylic Acid) as “Molecular Hydrogel” Templates. *Adv. Mater.* **2007**, *19* (3), 349–352.
- (17) Díez, I.; Pusa, M.; Kulmala, S.; Jiang, H.; Walther, A.; Goldmann, A. S.; Müller, A. H. E.; Ikkala, O.; Ras, R. H. A. Color Tunability and Electrochemiluminescence of Silver Nanoclusters. *Angew. Chem., Int. Ed.* **2009**, *48* (12), 2122–2125.
- (18) Gwinn, E. G.; O’Neill, P.; Guerrero, A. J.; Bouwmeester, D.; Fygenson, D. K. Sequence-Dependent Fluorescence of DNA-Hosted Silver Nanoclusters. *Adv. Mater.* **2008**, *20* (2), 279–283.
- (19) Patel, A. S.; Mohanty, T. Silver Nanoclusters in BSA Template: A Selective Sensor for Hydrogen Peroxide. *J. Mater. Sci.* **2014**, *49* (5), 2136–2143.

- (20) González, B. S.; Blanco, M. C.; López-Quintela, M. A. Single Step Electrochemical Synthesis of Hydrophilic/Hydrophobic Ag₂ and Ag₃ Blue Luminescent Clusters. *Nanoscale* **2012**, *4* (24), 7632–7635.
- (21) Zhou, Y.; Yu, Y.; Chai, Y.; Yuan, R. Electrochemical Synthesis of Silver Nanoclusters on Electrochemiluminescent Resonance Energy Transfer Amplification Platform for Apo-A1 Detection. *Talanta* **2018**, *181*, 32–37.
- (22) Ershov, B. G.; Janata, E.; Henglein, A. Growth of Silver Particles in Aqueous Solution: Long-Lived “Magic” Clusters and Ionic Strength Effects. *J. Phys. Chem.* **1993**, *97* (2), 339–343.
- (23) Ershov, B. G.; Henglein, A. Reduction of Ag⁺ on Polyacrylate Chains in Aqueous Solution. *J. Phys. Chem. B* **1998**, *102* (52), 10663–10666.
- (24) Xu, H.; Suslick, K. S. Sonochemical Synthesis of Highly Fluorescent Ag Nanoclusters. *ACS Nano* **2010**, *4* (6), 3209–3214.
- (25) Zhang, J.; Xu, S.; Kumacheva, E. Photogeneration of Fluorescent Silver Nanoclusters in Polymer Microgels. *Adv. Mater.* **2005**, *17* (19), 2336–2340.
- (26) Chakraborty, I.; Bag, S.; Landman, U.; Pradeep, T. Atomically Precise Silver Clusters as New SERS Substrates. *J. Phys. Chem. Lett.* **2013**, *4* (16), 2769–2773.
- (27) Ledo-Suarez, A.; Rivas, J.; Rodríguez-Abreu, C. F.; Rodríguez, M. J.; Pastor, E.; Hernandez-Creus, A.; Oseroff, S. B.; López-Quintela, M. A. Facile Synthesis of Stable Subnanosized Silver Clusters in Microemulsion. *Angew. Chem., Int. Ed.* **2007**, *46*, 8823–8827.
- (28) Mathew, A.; Sajanlal, P. R.; Pradeep, T. A Fifteen Atom Silver Cluster Confined in Bovine Serum Albumin. *J. Mater. Chem.* **2011**, *21* (30), 11205–11212.
- (29) Shen, Z.; Duan, H.; Frey, H. Water-Soluble Fluorescent Ag Nanoclusters Obtained from Multiarm Star Poly(Acrylic Acid) as “Molecular Hydrogel” Templates. *Adv. Mater.* **2007**, *19*, 349–352.
- (30) Guo, W.; Yuan, J.; Wang, E. Oligonucleotide-Stabilized Ag Nanoclusters as Novel Fluorescence Probes for the Highly Selective and Sensitive Detection of the Hg²⁺ Ion. *Chem. Commun.* **2009**, *23*, 3395–3397.
- (31) Wu, Z.; Lanni, E.; Chen, W.; Bier, M. E.; Ly, D.; Jin, R. High Yield, Large Scale Synthesis of Thiolate-Protected Ag₇ Clusters. *J. Am. Chem. Soc.* **2009**, *131* (46), 16672–16674.
- (32) Kennes, K.; Coutino-Gonzalez, E.; Martin, C.; Baekelant, W.; Roeyfaers, M. B. J.; Van der Auweraer, M. Silver Zeolite Composites-Based LEDs: A Novel Solid-State Lighting Approach. *Adv. Funct. Mater.* **2017**, *27* (14), 1606411.
- (33) Kunwar, P.; Hassinen, J.; Bautista, G.; Ras, R. H. A.; Toivonen, J. Direct Laser Writing of Photostable Fluorescent Silver Nanoclusters in Polymer Films. *ACS Nano* **2014**, *8* (11), 11165–11171.
- (34) Canioni, L.; Bellec, M.; Royon, A.; Bousquet, B.; Cardinal, T. 3D Optical Data Storage Using Third-Harmonic Generation in Silver Zinc Phosphate Glass. *Opt. Lett.* **2008**, *33* (4), 360–362.
- (35) Makarava, N.; Parfenov, A.; Baskakov, I. V. Water-Soluble Hybrid Nanoclusters with Extra Bright and Photostable Emissions: A New Tool for Biological Imaging. *Biophys. J.* **2005**, *89* (1), 572–580.
- (36) Fournier, R. Theoretical Study of the Structure of Silver Clusters. *J. Chem. Phys.* **2001**, *115* (5), 2165–2177.
- (37) Coutino-Gonzalez, E.; Baekelant, W.; Steele, J. A.; Kim, C. W.; Roeyfaers, M. B. J.; Hofkens, J. Silver Clusters in Zeolites: From Self-Assembly to Ground-Breaking Luminescent Properties. *Acc. Chem. Res.* **2017**, *50* (9), 2353–2361.
- (38) Bellec, M.; Royon, A.; Bourhis, K.; Choi, J.; Bousquet, B.; Treguer, M.; Cardinal, T.; Videau, J. J.; Richardson, M.; Canioni, L. 3D Patterning At the Nanoscale of Fluorescent Emitters in Glass. *J. Phys. Chem. C* **2010**, *114* (37), 15584–15588.
- (39) Royon, A.; Bourhis, K.; Bellec, M.; Papon, G.; Bousquet, B.; Deshayes, Y.; Cardinal, T.; Canioni, L. Silver Clusters Embedded in Glass as a Perennial High Capacity Optical Recording Medium. *Adv. Mater.* **2010**, *22* (46), 5282–5286.
- (40) Royon, A.; Petit, Y.; Papon, G.; Richardson, M.; Canioni, L. Femtosecond Laser Induced Photochemistry in Materials Tailored with Photosensitive Agents [Invited]. *Opt. Mater. Express* **2011**, *1* (5), 866.
- (41) Vangheluwe, M.; Liang, F.; Petit, Y.; Hée, P.; Ledemi, Y.; Thomas, S.; Fargin, E.; Cardinal, T.; Messaddeq, Y.; Canioni, L.; Vallée, R. Enhancement of Nanograting Formation Assisted by Silver Ions in a Sodium Gallophosphate Glass. *Opt. Lett.* **2014**, *39* (19), 5491.
- (42) De Cremer, G.; Sels, B. F.; Hotta, J. I.; Roeyfaers, M. B. J.; Bartholomeeusen, E.; Coutino-Gonzalez, E.; Valtchev, V.; De Vos, D. E.; Vosch, T.; Hofkens, J. Optical Encoding of Silver Zeolite Microcarriers. *Adv. Mater.* **2010**, *22* (9), 957–960.
- (43) Lin, H.; Imakita, K.; Rong Gui, S. C.; Fujii, M. Near Infrared Emission from Molecule-like Silver Clusters Confined in Zeolite A Assisted by Thermal Activation. *J. Appl. Phys.* **2014**, *116* (1), 013509.
- (44) Rothschild, M. A Roadmap for Optical Lithography. *Opt. Photonics News* **2010**, *21* (6), 26–31.
- (45) LaFratta, C. N.; Fourkas, J. T.; Baldacchini, T.; Farrer, R. A. Multiphoton Fabrication. *Angew. Chem., Int. Ed.* **2007**, *46* (33), 6238–6258.
- (46) Mueller, B. Additive Manufacturing Technologies – Rapid Prototyping to Direct Digital Manufacturing. *Assembly Automation* **2012**, *32*, DOI: 10.1108/aa.2012.03332baa.010.
- (47) Kunwar, P.; Xiong, Z.; Zhu, Y.; Li, H.; Filip, A.; Soman, P. Hybrid Laser Printing of 3D, Multiscale, Multimaterial Hydrogel Structures. *Adv. Opt. Mater.* **2019**, *7*, 1900656.
- (48) Anscombe, N. Direct Laser Writing. *Nat. Photonics* **2010**, *4* (1), 22–23.
- (49) Maruo, S.; Nakamura, O.; Kawata, S. Three-Dimensional Microfabrication with Two-Photon-Absorbed Photopolymerization. *Opt. Lett.* **1997**, *22* (2), 132.
- (50) Ostendorf, A.; Chichkov, B. N. Two-Photon Polymerization: A New Approach to Micromachining. *Photonics Spectra* **2006**, *40*, 72–79.
- (51) Kunwar, P.; Toivonen, J.; Kauranen, M.; Bautista, G. Third-Harmonic Generation Imaging of Three-Dimensional Microstructures Fabricated by Photopolymerization. *Opt. Express* **2016**, *24* (9), 9353.
- (52) Soman, P.; Zhang, W.; Umeda, A.; Zhang, Z. J.; Chen, S. Femtosecond Laser-Assisted Optoporation for Drug and Gene Delivery into Single Mammalian Cells. *J. Biomed. Nanotechnol.* **2011**, *7*, 334–341.
- (53) Xiong, Z.; Li, H.; Kunwar, P.; Zhu, Y.; Ramos, R.; McLoughlin, S.; Winston, T.; Ma, Z.; Soman, P. Femtosecond Laser Induced Denaturation within Cell-Laden Hydrogels Results in Cellular Alignment. *Biofabrication* **2019**, *11* (3), 035005.
- (54) Hribar, K. C.; Soman, P.; Warner, J.; Chung, P.; Chen, S. Light-Assisted Direct-Write of 3D Functional Biomaterials. *Lab Chip* **2014**, *14*, 268–275.
- (55) Do, M. T.; Nguyen, T. T. N.; Li, Q.; Benisty, H.; Ledoux-Rak, I.; Lai, N. D. Submicrometer 3D Structures Fabrication Enabled by One-Photon Absorption Direct Laser Writing. *Opt. Express* **2013**, *21* (18), 20964.
- (56) Farsari, M.; Filippidis, G.; Fotakis, C. Fabrication of Three-Dimensional Structures by Three-Photon Polymerization. *Opt. Lett.* **2005**, *30* (23), 3180.
- (57) Qin, X. H.; Torgersen, J.; Saf, R.; Mühleder, S.; Pucher, N.; Ligon, S. C.; Holthöner, W.; Redl, H.; Ovsianikov, A.; Stampfl, J.; Liska, R. Three-Dimensional Microfabrication of Protein Hydrogels via Two-Photon-Excited Thiol-Vinyl Ester Photopolymerization. *J. Polym. Sci., Part A: Polym. Chem.* **2013**, *51* (22), 4799–4810.
- (58) Oser, C. H. M. Microfabrication Through a Multimode Optical Fiber. *Opt. Express* **2018**, *26* (2), 1766–1778.
- (59) Kaehr, B.; Ertaş, N.; Nielson, R.; Allen, R.; Hill, R. T.; Plenert, M.; Shear, J. B. Direct-Write Fabrication of Functional Protein Matrixes Using a Low-Cost Q-Switched Laser. *Anal. Chem.* **2006**, *78* (9), 3198–3202.
- (60) Turunen, S.; Käpylä, E.; Lähteenmäki, M.; Ylä-Outinen, L.; Narkilähti, S.; Kellomäki, M. Direct Laser Writing of Microstructures for the Growth Guidance of Human Pluripotent Stem Cell Derived Neuronal Cells. *Opt. Lasers Eng.* **2014**, *55*, 197–204.

- (61) Sun, H. B.; Kawata, S. Two-Photon Photopolymerization and 3D Lithographic Microfabrication. *Adv. Polym. Sci.* **2006**, *170*, 169–273.
- (62) Yeong, W. Y.; Yu, H.; Lim, K. P.; Ng, K. L. G.; Boey, Y. C. F.; Subbu, V. S.; Tan, L. P. Multiscale Topological Guidance for Cell Alignment via Direct Laser Writing on Biodegradable Polymer. *Tissue Eng., Part C* **2010**, *16* (5), 1011–1021.
- (63) Paun, I. A.; Zamfirescu, M.; Mihailescu, M.; Luculescu, C. R.; Mustaciosu, C. C.; Dorobantu, I.; Calenic, B.; Dinescu, M. Laser Micro-Patterning of Biodegradable Polymer Blends for Tissue Engineering. *J. Mater. Sci.* **2015**, *50* (2), 923–936.
- (64) Danilevicius, P. Micro-Structured Polymer Scaffolds Fabricated by Direct Laser Writing for Tissue Engineering. *J. Biomed. Opt.* **2012**, *17* (8), 081405.
- (65) Padolskyte, V.; Malinauskas, M.; Gailevicius, D.; Jonušauskas, L.; Sakirzanovas, S.; Gadonas, R.; Staliunas, K.; Mizeikis, V.; Juodkakis, S.; Chatterjee, S. Fabrication of 3D Glass-Ceramic Micro-/Nano-Structures by Direct Laser Writing Lithography and Pyrolysis. *Adv. Fabr. Technol. Micro/Nano Opt. Photonics XI* **2018**, 1054416, 40.
- (66) Vaezi, M.; Seitz, H.; Yang, S. A Review on 3D Micro-Additive Manufacturing Technologies. *Int. J. Adv. Manuf. Technol.* **2013**, *67* (5–8), 1721–1754.
- (67) Kämpylä, E.; Sedláček, T.; Aydogan, D. B.; Viitanen, J.; Rypáček, F.; Kellomäki, M. Direct Laser Writing of Synthetic Poly(Amino Acid) Hydrogels and Poly(Ethylene Glycol) Diacrylates by Two-Photon Polymerization. *Mater. Sci. Eng., C* **2014**, *43*, 280–289.
- (68) Kaehr, B.; Scrymgeour, D. A. Direct-Write Graded Index Materials Realized in Protein Hydrogels. *Appl. Phys. Lett.* **2016**, *109* (12), 123701.
- (69) Sarig-Nadir, O.; Livnat, N.; Zajdman, R.; Shoham, S.; Seliktar, D. Laser Photoablation of Guidance Microchannels into Hydrogels Directs Cell Growth in Three Dimensions. *Biophys. J.* **2009**, *96* (11), 4743–4752.
- (70) Ovsianikov, A.; Mühleder, S.; Torgersen, J.; Li, Z.; Qin, X. H.; Van Vlierberghe, S.; Dubruel, P.; Holnthoner, W.; Redl, H.; Liska, R.; Stampfl, J. Laser Photofabrication of Cell-Containing Hydrogel Constructs. *Langmuir* **2014**, *30* (13), 3787–3794.
- (71) Marino, A.; Filippeschi, C.; Genchi, G. G.; Mattoli, V.; Mazzolai, B.; Ciofani, G. The Osteoprint: A Bioinspired Two-Photon Polymerized 3-D Structure for the Enhancement of Bone-like Cell Differentiation. *Acta Biomater.* **2014**, *10* (10), 4304–4313.
- (72) Ye, J.; Tan, H.; Wu, S.; Ni, K.; Pan, F.; Liu, J.; Tao, Z.; Qu, Y.; Ji, H.; Simon, P.; Zhu, Y. Direct Laser Writing of Graphene Made from Chemical Vapor Deposition for Flexible, Integratable Micro-Supercapacitors with Ultrahigh Power Output. *Adv. Mater.* **2018**, *30* (27), 1801384.
- (73) Kang, S. Y.; Evans, C. C.; Shukla, S.; Reshef, O.; Mazur, E. Patterning and Reduction of Graphene Oxide Using Femtosecond-Laser Irradiation. *Opt. Laser Technol.* **2018**, *103*, 340–345.
- (74) El-Kady, M. F.; Kaner, R. B. Direct Laser Writing of Graphene Electronics. *ACS Nano* **2014**, *8* (9), 8725–8729.
- (75) Gan, Z.; Cao, Y.; Gu, M. Direct Laser Writing of Three-Dimensional Narrow Bandgap and High Refractive-Index PbSe Structures in a Solution. *Opt. Express* **2013**, *21* (9), 11202.
- (76) Au, T. H.; Trinh, D. T.; Tong, Q. C.; Do, D. B.; Nguyen, D. P.; Phan, M.-H.; Lai, N. D. Direct Laser Writing of Magneto-Photonic Sub-Microstructures for Prospective Applications in Biomedical Engineering. *Nanomaterials* **2017**, *7* (5), 105.
- (77) Beliatas, M. J.; Martin, N. A.; Leming, E. J.; Silva, S. R. P.; Henley, S. J. Laser Ablation Direct Writing of Metal Nanoparticles for Hydrogen and Humidity Sensors. *Langmuir* **2011**, *27* (3), 1241–1244.
- (78) Dmitriev, P. A.; Makarov, S. V.; Milichko, V. A.; Mukhin, I. S.; Samusev, A. K.; Krasnok, A. E.; Belov, P. A. Direct Femtosecond Laser Writing of Optical Nanoresonators. *J. Phys.: Conf. Ser.* **2016**, *690* (1), 012021.
- (79) Tanaka, T.; Ishikawa, A.; Kawata, S. Two-Photon-Induced Reduction of Metal Ions for Fabricating Three-Dimensional Electrically Conductive Metallic Microstructure. *Appl. Phys. Lett.* **2006**, *88* (8), 081107.
- (80) Zhao, Y. Y.; Zheng, M. L.; Dong, X. Z.; Jin, F.; Liu, J.; Ren, X. L.; Duan, X. M.; Zhao, Z. S. Tailored Silver Grid as Transparent Electrodes Directly Written by Femtosecond Laser. *Appl. Phys. Lett.* **2016**, *108* (22), 221104.
- (81) He, G. C.; Zheng, M. L.; Dong, X. Z.; Jin, F.; Liu, J.; Duan, X. M.; Zhao, Z. S. The Conductive Silver Nanowires Fabricated by Two-Beam Laser Direct Writing on the Flexible Sheet. *Sci. Rep.* **2017**, *7*, 1–8.
- (82) Blasco, E.; Müller, J.; Müller, P.; Trouillet, V.; Schön, M.; Scherer, T.; Barner-Kowollik, C.; Wegener, M. Fabrication of Conductive 3D Gold-Containing Microstructures via Direct Laser Writing. *Adv. Mater.* **2016**, *28* (18), 3592–3595.
- (83) Stellacci, F.; Bauer, C. A.; Meyer-Friedrichsen, T.; Wenseleers, W.; Alain, V.; Kuebler, S. M.; Pond, S. J. K.; Zhang, Y.; Marder, S. R.; Perry, J. W. Laser and Electron-Beam Induced Growth of Nanoparticles for 2D and 3D Metal Patterning. *Adv. Mater.* **2002**, *14* (3), 194–198.
- (84) Kang, S. Y.; Vora, K.; Mazur, E. One-Step Direct-Laser Metal Writing of Sub-100 Nm 3D Silver Nanostructures in a Gelatin Matrix. *Nanotechnology* **2015**, *26* (12), 121001.
- (85) Bellec, M.; Royon, A.; Bousquet, B.; Bourhis, K.; Treguer, M.; Cardinal, T.; Richardson, M.; Canioni, L. Beat the Diffraction Limit in 3D Direct Laser Writing in Photosensitive Glass. *Opt. Express* **2009**, *17* (12), 10304.
- (86) Maurel, C.; Cardinal, T.; Bellec, M.; Canioni, L.; Bousquet, B.; Treguer, M.; Videau, J. J.; Choi, J.; Richardson, M. Luminescence Properties of Silver Zinc Phosphate Glasses Following Different Irradiations. *J. Lumin.* **2009**, *129* (12), 1514–1518.
- (87) Papon, G.; Royon, A.; Marquestaut, N.; Fargues, A.; Petit, Y.; Dussauze, M.; Rodriguez, V.; Cardinal, T.; Canioni, L. Direct Laser Writing of Efficient Effective Second Order Nonlinear Optical Properties in a Tailored Silver-Doped Phosphate Glass. *MATEC Web Conf.* **2013**, *8* (6), 02006.
- (88) Eaton, S. M.; Zhang, H.; Herman, P. R.; Yoshino, F.; Shah, L.; Bovatsek, J.; Arai, A. Y. Heat Accumulation Effects in Femtosecond Laser-Written Waveguides with Variable Repetition Rate. *Opt. Express* **2005**, *13* (12), 4708.
- (89) Sun, T.; Seff, K. Silver Clusters and Chemistry in Zeolites. *Chem. Rev.* **1994**, *94* (4), 857–870.
- (90) Kunwar, P.; Hassinen, J.; Bautista, G.; Ras, R. H. A.; Toivonen, J. Sub-Micron Scale Patterning of Fluorescent Silver Nanoclusters Using Low-Power Laser. *Sci. Rep.* **2016**, *6* (March), 6–11.
- (91) Kunwar, P.; Turquet, L.; Hassinen, J.; Ras, R. H. A.; Toivonen, J.; Bautista, G. Holographic Patterning of Fluorescent Microstructures Comprising Silver Nanoclusters. *Opt. Mater. Express* **2016**, *6* (3), 946.
- (92) Karimi, N.; Kunwar, P.; Hassinen, J.; Ras, R. H. A.; Toivonen, J. Micropatterning of Silver Nanoclusters Embedded in Polyvinyl Alcohol Films. *Opt. Lett.* **2016**, *41* (15), 3627–3630.
- (93) Bourhis, K.; Royon, A.; Bellec, M.; Choi, J.; Fargues, A.; Treguer, M.; Videau, J. J.; Talaga, D.; Richardson, M.; Cardinal, T.; Canioni, L. Femtosecond Laser Structuring and Optical Properties of a Silver and Zinc Phosphate Glass. *J. Non-Cryst. Solids* **2010**, *356* (44–49), 2658–2665.
- (94) Smetanina, E. O.; Chimier, B.; Petit, Y.; Royon, A.; Cardinal, T.; Canioni, L.; Duchateau, G. Laser Writing of Nonlinear Optical Properties in Silver-Doped Phosphate Glass. *Opt. Lett.* **2017**, *42* (9), 1688.
- (95) Chakraborty, I.; Pradeep, T. Atomically Precise Clusters of Noble Metals: Emerging Link between Atoms and Nanoparticles. *Chem. Rev.* **2017**, *117* (12), 8208–8271.
- (96) Zheng, J.; Nicovich, P. R.; Dickson, R. M. Highly Fluorescent Noble-Metal Quantum Dots. *Annu. Rev. Phys. Chem.* **2007**, *58* (1), 409–431.
- (97) Xu, H.; Suslick, K. S. Water-Soluble Fluorescent Silver Nanoclusters. *Adv. Mater.* **2010**, *22* (10), 1078–1082.
- (98) Dhanya, S.; Saumya, V.; Rao, T. P. Synthesis of Silver Nanoclusters, Characterization and Application to Trace Level

Sensing of Nitrate in Aqueous Media. *Electrochim. Acta* **2013**, *102*, 299–305.

(99) Yao, Q.; Chen, T.; Yuan, X.; Xie, J. Toward Total Synthesis of Thiolate-Protected Metal Nanoclusters. *Acc. Chem. Res.* **2018**, *51* (6), 1338–1348.

(100) Ghosh, A.; Pradeep, T. Synthesis of Atomically Precise Silver Clusters by Using the Miscibility Principle. *Eur. J. Inorg. Chem.* **2014**, *2014* (31), 5271–5275.

(101) Shang, L.; Dong, S. Facile Preparation of Water-Soluble Fluorescent Silver Nanoclusters Using a Polyelectrolyte Template. *Chem. Commun.* **2008**, *9*, 1088.

(102) Chakraborty, I.; Govindarajan, A.; Erusappan, J.; Ghosh, A.; Pradeep, T.; Yoon, B.; Whetten, R. L.; Landman, U. The Superstable 25 kDa Monolayer Protected Silver Nanoparticle: Measurements and Interpretation as an Icosahedral $\text{Ag}_{152}(\text{SCH}_2\text{CH}_2\text{Ph})_{60}$ Cluster. *Nano Lett.* **2012**, *12* (11), 5861–5866.

(103) Shang, L.; Dörlich, R. M.; Trouillet, V.; Bruns, M.; Ulrich Nienhaus, G. Ultrasmall Fluorescent Silver Nanoclusters: Protein Adsorption and Its Effects on Cellular Responses. *Nano Res.* **2012**, *5* (8), 531–542.

(104) Li, R.; Wang, C.; Bo, F.; Wang, Z.; Shao, H.; Xu, S.; Cui, Y. Microwave-Assisted Synthesis of Fluorescent Ag Nanoclusters in Aqueous Solution. *ChemPhysChem* **2012**, *13* (8), 2097–2101.

(105) Lu, W.; Ma, W.; Lu, J.; Li, X.; Zhao, Y.; Chen, G. Microwave-Assisted Synthesis of Glycopolymer-Functionalized Silver Nanoclusters: Combining the Bioactivity of Sugar with the Fluorescence and Cytotoxicity of Silver. *Macromol. Rapid Commun.* **2014**, *35* (8), 827–833.

(106) Diez, I.; Ras, R. H. A.; Kanyuk, M. I.; Demchenko, A. P. On Heterogeneity in Fluorescent Few-Atom Silver Nanoclusters. *Phys. Chem. Chem. Phys.* **2013**, *15* (3), 979–985.

(107) De Cremer, G.; Coutiño-Gonzalez, E.; Roeyfaers, M. B. J.; Moens, B.; Ollevier, J.; Van Der Auweraer, M.; Schoonheydt, R.; Jacobs, P. A.; De Schryver, F. C.; Hofkens, J.; De Vos, D. E.; Sels, B. F.; Vosch, T. Characterization of Fluorescence in Heat-Treated Silver-Exchanged Zeolites. *J. Am. Chem. Soc.* **2009**, *131* (8), 3049–3056.

(108) Maretti, L.; Billone, P. S.; Liu, Y.; Scaiano, J. C. Facile Photochemical Synthesis and Characterization of Highly Fluorescent Silver Nanoparticles. *J. Am. Chem. Soc.* **2009**, *131* (39), 13972–13980.

(109) Capadona, L. A. Photoactivated Fluorescence of Small Silver Nanoclusters and Their Relation to Raman Spectroscopy. Thesis, Georgia Institute of Technology, Atlanta, GA, 2004.

(110) Peyser-Capadona, L.; Zheng, J.; González, J. I.; Lee, T.-H.; Patel, S. A.; Dickson, R. M. Nanoparticle-Free Single Molecule Anti-Stokes Raman Spectroscopy. *Phys. Rev. Lett.* **2005**, *94* (5), 058301.

(111) Copp, S. M.; Faris, A.; Swasey, S. M.; Gwinn, E. G. Heterogeneous Solvatochromism of Fluorescent DNA-Stabilized Silver Clusters Precludes Use of Simple Onsager-Based Stokes Shift Models. *J. Phys. Chem. Lett.* **2016**, *7* (4), 698–703.

(112) Yu, J.; Patel, S. A.; Dickson, R. M. In Vitro and Intracellular Production of Peptide-Encapsulated Fluorescent Silver Nanoclusters. *Angew. Chem., Int. Ed.* **2007**, *46* (12), 2028–2030.

(113) Jiang, H.; Xu, G.; Sun, Y.; Zheng, W.; Zhu, X.; Wang, B.; Zhang, X.; Wang, G. A “Turn-on” Silver Nanocluster Based Fluorescent Sensor for Folate Receptor Detection and Cancer Cell Imaging under Visual Analysis. *Chem. Commun.* **2015**, *51* (59), 11810–11813.

(114) Gao, S.; Chen, D.; Li, Q.; Ye, J.; Jiang, H.; Amatore, C.; Wang, X. Near-Infrared Fluorescence Imaging of Cancer Cells and Tumors through Specific Biosynthesis of Silver Nanoclusters. *Sci. Rep.* **2015**, *4*, 1–6.

(115) Patel, S. A.; Richards, C. I.; Hsiang, J. C.; Dickson, R. M. Water-Soluble Ag Nanoclusters Exhibit Strong Two-Photon-Induced Fluorescence. *J. Am. Chem. Soc.* **2008**, *130* (35), 11602–11603.

(116) Xia, N.; Yang, J.; Wu, Z. Fast, High-Yield Synthesis of Amphiphilic Ag Nanoclusters and the Sensing of Hg^{2+} in Environmental Samples. *Nanoscale* **2015**, *7* (22), 10013–10020.

(117) Yuan, Z.; Cai, N.; Du, Y.; He, Y.; Yeung, E. S. Sensitive and Selective Detection of Copper Ions with Highly Stable Polyethylene-

neimine-Protected Silver Nanoclusters. *Anal. Chem.* **2014**, *86*, 419–426.

(118) Zhang, J. R.; Zeng, A. L.; Luo, H. Q.; Li, N. B. Fluorescent Silver Nanoclusters for Ultrasensitive Determination of Chromium(VI) in Aqueous Solution. *J. Hazard. Mater.* **2016**, *304*, 66–72.

(119) Li, Y.; Wang, X.; Chen, G.; Xu, S.; Xu, W. Fluorescent Silver Nanoclusters Embedded with Polymer Nanoparticles for Sensing Copper Ions. *Anal. Methods* **2013**, *5* (16), 3853–3857.

(120) Shang, L.; Dong, S. Sensitive Detection of Cysteine Based on Fluorescent Silver Clusters. *Biosens. Bioelectron.* **2009**, *24* (6), 1569–1573.

(121) Han, B.; Wang, E. Oligonucleotide-Stabilized Fluorescent Silver Nanoclusters for Sensitive Detection of Biothiols in Biological Fluids. *Biosens. Bioelectron.* **2011**, *26* (5), 2585–2589.

(122) Sharma, J.; Yeh, H. C.; Yoo, H.; Werner, J. H.; Martinez, J. S. Silver Nanocluster Aptamers: In Situ Generation of Intrinsically Fluorescent Recognition Ligands for Protein Detection. *Chem. Commun.* **2011**, *47*, 2294–2296.

(123) Guo, W.; Yuan, J.; Dong, Q.; Wang, E. Highly Sequence-Dependent Formation of Fluorescent Silver Nanoclusters in Hybridized DNA Duplexes for Single Nucleotide Mutation Identification. *J. Am. Chem. Soc.* **2010**, *132* (3), 932–934.

(124) Shah, P.; Cho, S. K.; Thulstrup, P. W.; Bhang, Y. J.; Ahn, J. C.; Choi, S. W.; Rørvig-Lund, A.; Yang, S. W. Effect of Salts, Solvents and Buffer on miRNA Detection Using DNA Silver Nanocluster (DNA/AgNCs) Probes. *Nanotechnology* **2014**, *25* (4), 045101.

(125) Haque, F.; Guo, P. RNA Nanotechnology and Therapeutics: Methods and Protocols. *Methods Mol. Biol.* **2015**, *1297*, 1.

(126) Mishchik, K.; Petit, Y.; Brasselet, E.; Royon, A.; Cardinal, T.; Canioni, L. Patterning Linear and Nonlinear Optical Properties of Photosensitive Glasses by Femtosecond Structured Light. *Opt. Lett.* **2015**, *40* (2), 201–204.

(127) Muhammed, M. A. H.; Aldeek, F.; Palui, G.; Trapiella-Alfonso, L.; Mattoussi, H. Growth of in Situ Functionalized Luminescent Silver Nanoclusters by Direct Reduction and Size Focusing. *ACS Nano* **2012**, *6* (10), 8950–8961.

(128) Udaya Bhaskara Rao, T.; Pradeep, T. Luminescent Ag_7 and Ag_8 Clusters by Interfacial Synthesis. *Angew. Chem., Int. Ed.* **2010**, *49* (23), 3925–3929.

(129) Chakraborty, I.; Kurashige, W.; Kanehira, K.; Gell, L.; Häkkinen, H.; Negishi, Y.; Pradeep, T. $\text{Ag}_{44}(\text{SeR})_{30}$: A Hollow Cage Silver Cluster with Selenolate Protection. *J. Phys. Chem. Lett.* **2013**, *4* (19), 3351–3355.

(130) Liu, T.; Su, Y.; Song, H.; Lv, Y. Microwave-Assisted Green Synthesis of Ultrasmall Fluorescent Water-Soluble Silver Nanoclusters and Its Application in Chiral Recognition of Amino Acids. *Analyst* **2013**, *138* (21), 6558–6564.

(131) Zhang, J.; Yuan, Y.; Wang, Y.; Sun, F.; Liang, G.; Jiang, Z.; Yu, S. H. Microwave-Assisted Synthesis of Photoluminescent Glutathione-Capped Au/Ag Nanoclusters: A Unique Sensor-on-a-Nanoparticle for Metal Ions, Anions, and Small Molecules. *Nano Res.* **2015**, *8* (7), 2329–2339.

(132) Chakraborty, I.; Udayabhaskararao, T.; Pradeep, T. High Temperature Nucleation and Growth of Glutathione Protected $\square\text{Ag}_{75}$ Clusters. *Chem. Commun.* **2012**, *48* (54), 6788–6790.

(133) Linnert, T.; Mulvaney, P.; Henglein, A.; Weller, H. Long-Lived Nonmetallic Silver Clusters in Aqueous Solution: Preparation and Photolysis. *J. Am. Chem. Soc.* **1990**, *112* (12), 4657–4664.

(134) Henglein, A. Non-Metallic Silver Clusters in Aqueous Solution: Stabilization and Chemical Reactions. *Chem. Phys. Lett.* **1989**, *154* (5), 473–476.

(135) Dhanalakshmi, L.; Udayabhaskararao, T.; Pradeep, T. Conversion of Double Layer Charge-Stabilized $\text{Ag}@$ citrate Colloids to Thiol Passivated Luminescent Quantum Clusters. *Chem. Commun.* **2012**, *48* (6), 859–861.

(136) Abou Khalil, A.; Bérubé, J. P.; Danto, S.; Desmoulin, J. C.; Cardinal, T.; Petit, Y.; Vallée, R.; Canioni, L. Direct Laser Writing of a New Type of Waveguides in Silver Containing Glasses. *Sci. Rep.* **2017**, *7* (1), 1–9.

- (137) De Cremer, G.; Antoku, Y.; Roeyfaers, M. B. J.; Sliwa, M.; Van Noyen, J.; Smout, S.; Hofkens, J.; De Vos, D. E.; Sels, B. F.; Vosch, T. Photoactivation of Silver-Exchanged Zeolite A. *Angew. Chem., Int. Ed.* **2008**, *47* (15), 2813–2816.
- (138) Vangheluwe, M.; Petit, Y.; Marquestaut, N.; Corcoran, A.; Fargin, E.; Vallée, R.; Cardinal, T.; Canioni, L. Nanoparticle Generation inside Ag-Doped LBG Glass by Femtosecond Laser Irradiation. *Opt. Mater. Express* **2016**, *6* (3), 743.
- (139) Lee, E.; Petit, Y.; Brasselet, E.; Cardinal, T.; Park, S.-H.; Canioni, L. Sub-Diffraction-Limited Fluorescent Patterns by Tightly Focusing Polarized Femtosecond Vortex Beams in a Silver-Containing Glass. *Opt. Express* **2017**, *25* (9), 10565–10573.
- (140) Yokota, R.; Imagawa, H. Radiophotoluminescent Centers in Silver-Activated Phosphate Glass. *J. Phys. Soc. Jpn.* **1967**, *23*, 1038–1048.
- (141) Zhao, J.; Lin, J.; Zhang, W.; Zhang, S.; Zhao, G.; Cai, W. An Optical Investigation of Silver Nanoclusters Composite Soda-Lime Glass Formed by Electric Field Assisted Diffusion. *J. Wuhan Univ. Technol., Mater. Sci. Ed.* **2017**, *32* (2), 338–344.
- (142) Petit, Y.; Danto, S.; Guérineau, T.; Abou Khalil, A.; Le Camus, A.; Fargin, E.; Duchateau, G.; Bérubé, J. P.; Vallée, R.; Messaddeq, Y.; Cardinal, T.; Canioni, L. On the Femtosecond Laser-Induced Photochemistry in Silver-Containing Oxide Glasses: Mechanisms, Related Optical and Physico-Chemical Properties, and Technological Applications. *Adv. Opt. Technol.* **2018**, *7* (5), 291–309.
- (143) Papon, G.; Petit, Y.; Marquestaut, N.; Royon, A.; Dussauze, M.; Rodriguez, V.; Cardinal, T.; Canioni, L. Fluorescence and Second-Harmonic Generation Correlative Microscopy to Probe Space Charge Separation and Silver Cluster Stabilization during Direct Laser Writing in a Tailored Silver-Containing Glass. *Opt. Mater. Express* **2013**, *3* (11), 1855.
- (144) Choi, J.; Bellec, M.; Royon, A.; Bourhis, K.; Papon, G.; Cardinal, T.; Canioni, L.; Richardson, M. Three-Dimensional Direct Femtosecond Laser Writing of Second-Order Nonlinearities in Glass. *Opt. Lett.* **2012**, *37* (6), 1029.
- (145) Marquestaut, N.; Petit, Y.; Royon, A.; Mounaix, P.; Cardinal, T.; Canioni, L. Three-Dimensional Silver Nanoparticle Formation Using Femtosecond Laser Irradiation in Phosphate Glasses: Analogy with Photography. *Adv. Funct. Mater.* **2014**, *24* (37), 5824–5832.
- (146) Danto, S.; Désévéday, F.; Petit, Y.; Desmoulin, J. C.; Abou Khalil, A.; Strutynski, C.; Dussauze, M.; Smektala, F.; Cardinal, T.; Canioni, L. Photowritable Silver-Containing Phosphate Glass Ribbon Fibers. *Adv. Opt. Mater.* **2016**, *4* (1), 162–168.
- (147) Smetanina, E.; Chimier, B.; Petit, Y.; Varkentina, N.; Fargin, E.; Hirsch, L.; Cardinal, T.; Canioni, L.; Duchateau, G. Modeling of Cluster Organization in Metal-Doped Oxide Glasses Irradiated by a Train of Femtosecond Laser Pulses. *Phys. Rev. A: At., Mol., Opt. Phys.* **2016**, *93* (1), 013846.
- (148) Guérineau, T.; Loi, L.; Petit, Y.; Danto, S.; Fargues, A.; Canioni, L.; Cardinal, T. Structural Influence on the Femtosecond Laser Ability to Create Fluorescent Patterns in Silver-Containing Sodium-Gallium Phosphate Glasses. *Opt. Mater. Express* **2018**, *8* (12), 3748.
- (149) Petit, Y.; Park, C.-H.; Mok, J.-M.; Smetanina, E.; Chimier, B.; Duchateau, G.; Cardinal, T.; Canioni, L.; Park, S.-H. Ultrashort Laser Induced Spatial Redistribution of Silver Species and Nano-Patterning of Etching Selectivity in Silver-Containing Glasses. *Opt. Express* **2019**, *27* (10), 13675.
- (150) Petit, Y.; Mishchik, K.; Varkentina, N.; Marquestaut, N.; Royon, A.; Manek-Honninger, I.; Cardinal, T.; Canioni, L. Dual-Color Control and Inhibition of Direct Laser Writing in Silver-Containing Phosphate Glasses. *Opt. Lett.* **2015**, *40* (17), 4134–4137.
- (151) de Castro, T.; Fares, H.; Khalil, A. A.; Laberdesque, R.; Petit, Y.; Strutynski, C.; Danto, S.; Jubera, V.; Ribeiro, S. J. L.; Nalin, M.; Cardinal, T.; Canioni, L. Femtosecond Laser Micro-Patterning of Optical Properties and Functionalities in Novel Photosensitive Silver-Containing Fluorophosphate Glasses. *J. Non-Cryst. Solids* **2019**, *517* (May), 51–56.
- (152) Royon, A.; Bourhis, K.; Béchou, L.; Cardinal, T.; Canioni, L.; Deshayes, Y. Durability Study of a Fluorescent Optical Memory in Glass Studied by Luminescence Spectroscopy. *Microelectron. Reliab.* **2013**, *53* (9–11), 1514–1518.
- (153) Altantzis, T.; Coutino-Gonzalez, E.; Baekelant, W.; Martinez, G. T.; Abakumov, A. M.; Van Tendeloo, G.; Roeyfaers, M. B. J.; Bals, S.; Hofkens, J. Direct Observation of Luminescent Silver Clusters Confined in Faujasite Zeolites. *ACS Nano* **2016**, *10* (8), 7604–7611.
- (154) Morgan, D. J. An Introduction to Zeolite Molecular Sieves. *Mineral. Mag.* **1989**, *53*, 662–662.
- (155) Bauer, W. Methacrylic Acid and Derivatives. *Ullmann's Encyclopedia of Industrial Chemistry* **2011**, 413–454.
- (156) Mulko, L. E.; Rossa, M.; Aranguren-Abrate, J. P.; Pino, G. A. Micropatterning of Fluorescent Silver Nanoclusters in Polymer Films by Laser Interference. *Appl. Surf. Sci.* **2019**, *485*, 141–146.
- (157) Ghildiyal, P.; Yang, Y.; Zachariah, M. R.; Kline, D. J.; Holdren, S. Ultrafast, Scalable Laser Photothermal Synthesis and Writing of Uniformly Dispersed Metal Nanoclusters in Polymer Films. *Nanoscale* **2019**, *11*, 13354–13365.
- (158) Bitarafan, M.; Suomala, S.; Toivonen, J. Sub-Microwatt Direct Laser Writing of Fluorescent Gold Nanoclusters in Polymer Films. *Opt. Mater. Express* **2020**, *10* (1), 138–148.
- (159) Shao, C.; Yuan, B.; Wang, H.; Zhou, Q.; Li, Y.; Guan, Y.; Deng, Z. Eggshell Membrane as a Multimodal Solid State Platform for Generating Fluorescent Metal Nanoclusters. *J. Mater. Chem.* **2011**, *21* (9), 2863–2866.